

POLITECNICO DI MILANO

Corsi di Laurea Magistrale in Ingegneria Biomedica



THE EFFECT OF PROTEINS ON HYDROXYAPATITE DISSOLUTION

Supervisor: Prof. Stefano Servi

Tesi di laurea : Maryam Bolhassani, Matricola: 752527

ANNO ACCADEMICO 2012-2013

ABSTRACT

Studying proteins used to retard bone (or hydroxyapatite) dissolution could provide important design principles for the development of decalcification inhibitors and at the same time calcification promoters in orthopedics, cardiology, urology, and dentistry.

The aim of this research is to study the effect of proteins known to have specific binding activity on hydroxyapatite (HA) dissolution. Statherin and osteopontin have been taken as reference proteins and synthetic HA as model substrate. Since HA hydrolysis produces protons in solution, a pH-stat assay has been set up in order to follow and compare HA dissolution in the presence and the absence of model peptides. The effect of synthetic peptides corresponding to amino acid 220-235 and amino acid 65-80 of rat bone OPN have initially been considered. Due to the relevance of the presence of the phosphate group in calcium binding, OPN220-235 was synthesized in triphosphorylated (P3) and nonphosphorylated (P0) forms; OPN65-80 was synthesized in monophosphorylated (P-OPAR) and nonphosphorylated (OPAR) forms. Following the observation that highly acidic and phosphorylated peptides showed the most significant HA dissolution inhibition, also oligomers of asp and glu were prepared and tested. The substrate concentrations required to obtain 50% dissolution inhibition (IC_{50}) were measured and compared: the most significant values was with P3, 6 [$\mu\text{g/ml}$], followed by P-OPAR, 16 [$\mu\text{g/ml}$], OPAR, 22 [$\mu\text{g/ml}$], P0 > 75 [$\mu\text{g/ml}$]. Poly -L-aspartic acid (MW=2,320), and poly -L-glutamic acid (MW=2,600), tested because of the significant affinity of polyanions to HA surface showed interesting inhibition properties. The corresponding (IC_{50}) were: poly-Asp, 13 [$\mu\text{g/ml}$]; Poly-Glu, [18 $\mu\text{g/ml}$]. In an attempt to correlate the inhibition activity with the secondary structure of the peptides, structural informations were collected from their CD spectra. The secondary structure of these polyanions was investigated at 37°C in P buffer at pH [5.25].

We found that poly-Asp was mostly disordered compared with the poly- Glu with the same length and contained roughly 20% poly-proline II helix. P3, has been shown to be one of the strong inhibitor of HA dissolution.

In addition, the effects of statherin and DR9, which is 9-residue peptide derived from the N-terminal of the statherin have been studied. The IC_{50} measured were: statherin, 25 [μ M]; DR9, 13 [μ M]. DR9 was observed to have high affinity to HA surface compare to the statherin.

In conclusion it has been shown that peptides structurally derived from natural salivary proteins and bone proteins are able to adsorb to hydroxyapatite surfaces and induce a decrease in the rate of dissolution of HA which strongly depends on their chemical structure. Since OPN and statherin possess relatively high proportions of aspartic acid, glutamic acid and phosphorylated serine residues one can assume that a combination of acidic residues and post-translational phosphorylation strongly influence the biomineral adsorption. The presence of the negative charges is imperative in the ability of acidic protein and peptides to adsorb to the HA surface and prevent the dissolution of HA.

English Keywords: hydroxyapatite, protein, osteopontin, pH-Stat method, polyanion, dissolution, phosphoprotein, statherin, inhibitor, concentration

Italian Keywords: idrossiapatite, proteine, osteopontina, pH-Stat metodo, polielettrolita, dissoluzione, fosfoproteina, staterina, inibitore, concentrazione

ACKNOWLEDGEMENT

First of all I would like to express my gratitude to my advisor, Professor Graeme Hunter at the School of Dentistry, the University of Western Ontario, for his supervision, advice, guidance, and many enlightening discussions and most especially his patience when I was struggling. Needless to say, without him I would have no thesis. Above all and the most needed, he provided me unflinching encouragement and support in various ways. It has been a real privilege to work under the guidance of a person of his stature. His truly scientist intuition has made him as a constant oasis of ideas and passions in science, which exceptionally inspire and enrich my growth as a student want to be.

Many thanks to Professor Stefano Servi as my thesis advisor, at the chemistry department, Polytechnic University of Milan, for the valuable comments and suggestions which have led to significant improvement on this work.

Many thanks to my Professor Alberto Redaelli, who supported me, and without his help I would not be able to present my thesis. I would also like to thank Professor Harvey Goldberg for his guidance through the course of this work.

Words fail me to express my appreciation to my husband Behnam whose dedication, love and persistent confidence in me, has taken the load off my shoulder. I would also like to thank my parents for their support and encouragement over these years.

Last, but not least, I would like to thank all my labmates/friends: past and present members of Dr. Graeme Hunter and Dr. Harvey Goldberg laboratory in the Schulich School of Medicine and Dentistry at Western University of Ontario, Canada (UWO) , for their kindness and for the part

they play in making UWO such an attractive place in which to work and live. To everyone involved, thank you.

TABLE OF CONTENTS

ABSTRACT	i
ACKNOWLEDGMENT	iii
LIST OF TABLE	3
LIST OF FIGURE	4
LIST OF ABBREVIATION	6

Chapter one-Literature Review

1.1	Introduction	9
1.1.1	The effect of proteins on hydroxyapatite dissolution	9
1.1.2	SIBLING Proteins	11
1.1.2.1	Introduction to osteopontin	13
1.1.3	Salivary Protein	16
1.1.1.3	Introduction to statherin	17
1.2	Protein crystal interaction	19
1.3	Purpose of Thesis	23

Chapter two- pH-Stat method and dissolution studies

2.1	pH-Stat method and dissolution	25
2.2	Material and method	30
2.2.1	Chemical and reagent	30

2.2.2	Synthesis of hydroxyapatite seed crystal	31
2.2.3	Characterization of synthesized hydroxyapatite seed crystal	31
2.3	Dissolution assay	32

Chapter three-Protein inhibitory potency toward HA

3.1	Material and method	36
3.1.1	Chemical and reagent	36
3.1.2	Protein expression/purification and peptides synthesis /purification	38
3.1.3	Peptides secondary structure analysis	38
3.2	Inhibition of HA dissolution by OPN-derived peptides and statherin	40
3.3	Comparison between inhibitory potency of poly- Asp and poly-Glutamic	48
3.4	Discussion	54

REFERENCES

LIST OF TABLE

Table 1.	Naturally occurring statherin peptides found in AEP.....	15
Table 2	Chemical and Reagents chapter 2.....	30
Table 3.	Chemical and Reagents chapter 3.....	36
Table 4.	Summary of the average fractional secondary structure of OPN-derived peptides	39
Table 5.	Summary of pH-Stat method dissolution result.....	45

LIST OF FIGURE

Figure 1.	Amino acid sequence of statherin.....	15
Figure 2.	pH-Stat Titration Workstation.....	30
Figure 3.	HCl addition required to maintain constant pH during dissolution.....	36
Figure 4.	Rate of HA dissolution in the presence P0.....	42
Figure 5.	VHCl addition against P0 Concentration ($\mu\text{g/ml}$).....	42
Figure 6.	Rate of HA dissolution in the presence of P3.....	43
Figure 7.	VHCl addition against P3 peptide Concentration ($\mu\text{g/ml}$).....	43
Figure 8.	Rate of HA dissolution in the presence of OPAR.....	44
Figure 9.	VHCl addition against OPAR peptide Concentration ($\mu\text{g/ml}$).....	44
Figure 10.	Rate of HA dissolution in the presence of P-OPAR.....	45
Figure 11.	VHCl addition against P-OPAR peptide Concentration ($\mu\text{g/ml}$).....	45
Figure 12.	Rate of HA dissolution in the presence of DR9.....	46
Figure 13.	VHCl addition against DR9 peptide Concentration ($\mu\text{g/ml}$).....	46
Figure 14.	Rate of HA dissolution in the presence of Statherin.....	47
Figure 15.	VHCl addition against Statherin peptide Concentration ($\mu\text{g/ml}$).....	47
Figure 16.	Rate of HA dissolution in the presence of poly-Glu.....	50
Figure 17.	VHCl addition against poly-Glu peptide Concentration ($\mu\text{g/ml}$).....	50

Figure 18. Rate of HA dissolution in the presence of poly-Asp.....51

Figure 19. VHCl addition against poly-Asp peptide Concentration ($\mu\text{g/ml}$)....51

Figure 20. CD spectra of poly-Asp and poly-Glu dissolved in PO_4 buffer.....53

LIST OF ABBREVIATIONS

AEP	Acquired enamel pellicle
BSP	Bone sial protein
CD	Circular dichroism spectroscopy
DMP1	Dentin matrix protein 1
DSSP	Dentin sialophosphoprotein
ECM	Extracellular matrix
D	Aspartic acid
E	Glutamic acid
EAI	Equilibrium adsorption isotherm
ITC	Isothermal Titration Calorimetry
HA	Hydroxyapatite
K	Lysine
P	Proline
PTMs	Post-translational modifications
M	Methionine
MEPE	Matrix extracellular phosphoglycoprotein
MW	Molecular weight
S	Serine
SIBLING	Small Integrin-Binding LIgand, N-linked Glycoprotein
STATH	Statherin

OPN	Osteopontin
Q	Glutamine
RGD	Arginine-Glycine-Aspartic acid

Chapter One. Literature Review

1.1 Introduction

1.1.1 The effect of proteins on hydroxyapatite dissolution

Demineralization is the process of loss of the mineral phase of the hard tissues of living organisms [1]. Hard tissues are composed of insoluble calcium salts of carbonate, silicate and phosphate ions. The presence of the minerals depends on the chemistry of the environment in which they are formed and on factors such as the temperature of the aquatic environment and the presence of foreign ions. Bones and teeth consist largely of an inorganic calcium phosphate mineral approximated by hydroxyapatite (HA), $\text{Ca}_{10}(\text{PO}_4)_6(\text{OH})_2$, and matrix proteins. Pure HA never occurs in biological systems. However, due to the chemical similarities to bone and teeth mineral, HA is widely used as a coating on orthopedic (e.g., hip joint prosthesis) and dental implants [2]. The apatites found in tooth enamel, dentin and bone have slightly different compositions and therefore these tissues have different physical and mechanical properties. Dental enamel is the most highly mineralized and hardest biological tissue. It is composed of approximately 96% mineral, 3% water, and 1% organic matter (mostly non-collagenous protein) by weight [3]. The mineral is non-stoichiometric calcium hydroxyapatite and *in vivo* its dissolution in acids leads to the pathological conditions of dental erosion and caries. The dissolution of dental enamel in acidic solution is a function of several factors, including calcium, phosphate and acid concentration. . Enamel will dissolve if it is in a solution that is undersaturated with respect to HA. In the mouth, that will happen if the pH falls to <5.5 (the “critical pH”).

Dental caries, otherwise known as tooth decay, is one of the most prevalent chronic diseases of people worldwide; individuals are susceptible to this disease throughout their lifetime [4]. It forms through a complex interaction over time between acid-producing bacteria, particularly mutans streptococci and possibly lactobacilli, that ferment dietary carbohydrates [5]. This occurs within a bacteria-laden gelatinous material called dental plaque that adheres to tooth surfaces. A variety of carbohydrates provide substrates for these organisms to grow on and the waste products of their metabolism - acids - initiate the tooth decay process by dissolving tooth enamel. The acid attacks the tooth enamel and gradually dissolves it. However the demineralization process is offset by the repair process known as remineralization. The balance between remineralization and demineralization determines whether caries occurs. pH in oral environment varies from near neutral to ≤ 5 . Acidic pH levels (which are usually brought about by acids produced by locally colonized bacteria on enamel surface) lead to undersaturated state of saliva, thereby inducing enamel dissolution.[6]

It is believed that a variety of proteins function to prevent biomineralization and demineralization by adsorbing onto the crystal surfaces. [7] For instance, saliva forms a thin biofilm, on soft and hard oral tissues. [8] The salivary proteins such as statherin, proline-rich phosphoproteins (PRPs), histatins and cystatins are important stabilizers of human saliva that is supersaturated with respect to most calcium phosphate salts including hydroxyapatite. [9] This supersaturation is crucial for the integrity of the teeth since it provides a reparative environment [10]. These proteins electively adsorb on the HA surface forming a protective salivary biofilm called the 'pellicle' or acquired enamel pellicle (AEP) on tooth surface [11]. This film acts as a selective permeable barrier that acts as a defence against enamel demineralization and provides a medium through which fluoride, calcium; and phosphate are delivered during remineralization. It

has been suggested that statherin is the first salivary protein that binds to a cleansed enamel surface after tooth brushing and consider important in forming the AEP on tooth surfaces and delaying diffusion [12].

Moreover, phosphorylated proteins and peptides have been shown to have strong affinity to the hydroxyapatite surface [13]. The common characteristic of all proteins that exhibit a thermodynamic adsorption process is to possess regions of concentrated negative charge, whether due to clusters of phosphorylated or anionic amino acid residues or both. Several studies have been directed towards the significance of acidic amino-acid residues in mineral-binding proteins since many members of this class are poly-anionic [14]. These proteins possess relatively high proportions of aspartic acids, glutamic acid, serine and phosphorylated residues and they have a high affinity for the HA surface[15].

As a result, The aim of this research is to understand how different proteins adsorb to the hydroxyapatite surface and inhibit the dissolution of the crystal. The proteins of most interest to this research are osteopontin (OPN) and statherin. We have tested the effect of synthetic peptides corresponding to amino acid sequence of rat bone OPN and salivary protein using pH-Stat dissolution assay.

1.1.2 Salivary Proteins

Dental caries is a dynamic process since periods of demineralization alternate with periods of remineralization through the action of fluoride, calcium and phosphate contained in oral fluids. As a result the main contributing factor for caries is an imbalance of mineral between the tooth surface and its environment. The process of dental caries is dependent upon biological factors

that are present within the saliva and dental plaque. There are many different agents within saliva and plaque that serve to protect the tooth surface against caries development. Salivary flow rate, buffering capacity, antimicrobial activity, microorganism aggregation and clearance from the oral cavity, immune surveillance, and calcium and phosphate-binding proteins all interact to inhibit or reverse demineralization of exposed tooth surfaces [16], [17]. Cariogenic bacteria levels within the saliva and plaque determine whether caries will occur or not, and the concentration in saliva and plaque are intimately related to the type of carbohydrate ingestion and the frequency of ingestion, as well as the oral hygiene practiced by the individual. [5]

Salivary fluid is an exocrine secretion consisting of approximately 99% water, containing a variety of electrolytes (sodium, potassium, calcium, chloride, magnesium, bicarbonate, phosphate) and proteins, represented by enzymes, immunoglobulins and other antimicrobial factors, mucosal glycoproteins, traces of albumin and some polypeptides and oligopeptides of importance to oral health. It also contains glucose, urea and NH_3 [18]. The components interact and are responsible for the various functions attributed to saliva. A major protective function results from the salivary role in maintenance of the ecological balance in the oral cavity via: (1) aggregation and reduced adherence by both immunological and non-immunological means; and (2) direct antibacterial activity [19]. Furthermore, saliva is effective in maintaining pH in the oral cavity, contributes to the regulation of plaque pH, and helps neutralize acids reflux from the esophagus. Secretion of saliva is under control of the autonomic nervous system, which controls both the volume and type of saliva secreted [20]. It contains a spectrum of immunologic and non-immunologic proteins with antibacterial properties [21]. Thus, it has been suggested that saliva can be used for monitoring oral health, including periodontal diseases [22] and to assess

caries risk, as well as overall systemic health. Saliva has been found to contain biomarkers for cancer as well as bacterial and viral diseases [11].

It has been shown that salivary protein such as the proline-rich proteins and statherin inhibit the spontaneous precipitation of calcium phosphate salts and the growth of hydroxyapatite crystals on the tooth surface [23],[24]. They favor oral structure lubrication, and it is probable both are important in the formation of acquired film. Another function proposed for the proline-rich proteins is the capacity to selectively mediate bacterial adhesion to tooth surfaces. Thus, it is important to gain an understanding of how to utilize recent technological advances in dental research for predicting, monitoring, and preventing the development of oral diseases by investigating the diagnostic and therapeutic role of salivary proteins.

1.1.2.1 Introduction to Statherin

The most interesting protein of saliva for this study is statherin which is the first salivary protein to bind to a cleansed enamel surface after tooth brushing. Statherin is involved in the management of Ca^{2+} in the oral environment by binding calcium ions. This protein is a 43-amino-acid peptide (molecular weight=5380 Daltons) with a typical range of concentration in human saliva of 10-40 μM . In humans, statherin is encoded by the STATH gene. This salivary protein is produced by the acinar cells of the parotid and submandibular salivary glands and contains a tyrosine-rich region and vicinal phosphoserines in its primary structure [25]. The primary amino acid sequence of this amphipathic protein; is characterized by a negatively charged N terminus consisting of a DSSEEEK sequence, in which the serines are post-

translationally phosphorylated. It is considered likely that negative charge density and the α -helical conformation at the N-terminal region of statherin are important for its interaction with HA surfaces [26]. Its primary structure, reported by Schlesinger and Hay, shows a high charge asymmetry, in which a significant number of negatively charged residues are localized in the N-terminal region, whereas the C-terminal contains mainly uncharged residues[27], [17]. The secondary structure of statherin in 50% trifluoroethanol/water mixtures was determined to consist of an α -helical structure at the N-terminal region (residues Asp1–tyr16), a polyproline type II helix in the intermediate region (residues Gly19–Gln35) and a 3_{10} helix in the C-terminal region (residues Pro36–Phe43) [28].

Table 1. Naturally occurring statherin peptides found in AEP. DR-9/2 is synthetic non phosphorylated

Statherin peptide	Name	No. of residues	M ^r	Presence
DSpSpEEKFLR	DR-9	9	1270.1	In vivo AEP
DSSEEKFLR	DR-9/2	9	1110.2	Synthetic, non phosphorylated
GYGYGPYQPVPPE	GE-12	12	1326.4	In vivo AEP
IGRFGYGYGPYQPVPPEQP	IP-18	18	2025.2	In vivo AEP
GPYQPVPPEQPLYPQPYQPQ	GQ-19	19	2226.4	In vivo AEP
IGRFGYGYGPYQPVPPEQPLYPQPYQPQYQQYT	IT-32	32	3981.4	In vivo AEP

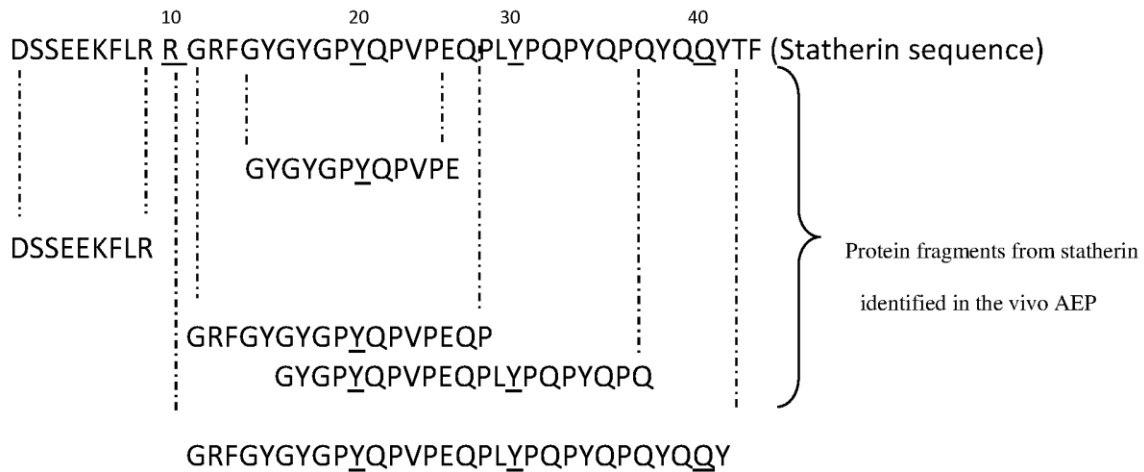


Fig 1. Amino acid sequence of statherin. The peptide fragments identified by LC-ESI-MS/MS are aligned below the protein sequence. Note the almost full coverage of statherin obtained with the exception of Arg10 and Phe43 (boxed). Siqueira W .L. *et al.*, 2009

1.1.3 SIBLING Proteins

The extracellular matrix (ECM) of bone and dentin contains several non-collagenous proteins [29]. One category of non-collagenous protein is termed the SIBLING (Small Integrin-Binding Ligand, N-linked Glycoprotein) family, which includes osteopontin (OPN), bone sialoprotein (BSP), dentin matrix protein 1 (DMP1), dentin sialophosphoprotein (DSPP), and matrix extracellular phosphoglycoprotein (MEPE). These polyanionic SIBLING proteins are believed to play key biological roles in the mineralization of bone and dentin [30],[29]. The genes coding for members of the SIBLING protein family are similarly organized and located on human chromosome 4q21-23 [31], [32]. These proteins share several common features including an Arg-Gly-Asp (RGD) cell-binding/signaling motif, acidic nature and presence of post-translational modifications such as phosphorylation and glycosylation. SIBLING proteins are abundant in mineralized tissues and supersaturated body fluids such as urine and breast milk suggesting that they possess important roles in both physiological and pathological forms of calcification. Although the specific mechanisms involved in controlling bone and dentin formation are still unknown, it is clear that some functions of the SIBLING family members are dependent on the nature and extent of post-translational modifications (PTMs), such as phosphorylation, glycosylation, and proteolytic processing, since these PTMs would have significant effects on their structure. SIBLING proteins have been found to be significantly upregulated in many tumours that exhibit tendencies to calcify and/or metastasize to bone [33].

1.1.3.1 Introduction to OPN

The protein of most interest to this work is osteopontin (OPN) which is a highly post translationally modified protein of approximately 300 residues containing RGD cell-binding motif and conserved poly-Asp region. OPN is post-translationally modified by phosphorylation, sulfation and glycosylation in a tissue-specific manner [34]. The primary sequence of osteopontin reveals a copious amount of charged residues, few hydrophobic residues and a high proportion of disorder-promoting residues [35], [36]. Mammalian osteopontins are identical in approximately 40% of their amino acid residues. OPN is expressed by a diverse array of tissues and found in all body fluids. Early studies revealed that in addition to bone, OPN is expressed in tissues such as the kidney, ovary and uterus. Subsequently, OPN was shown to be secreted by epithelial cells and present in biological fluids such as plasma, milk, saliva and urine.

A comparison of human and mouse OPNs reveals they are identical at approximately 63% of their amino acid positions. Serine residues are among the most highly conserved (24%) followed by the acidic residues aspartate 19% and glutamic 17%. The high prevalence of conserved acidic suggests negative charge may play an important role in osteopontin function. The conservation of serine residues even in less well-conserved areas of OPN suggests site-specific phosphorylation may be critical for the function of protein. Several studies suggested that OPN is disordered [37]. Several studies have reported lack of structure using circular dichroism OPN has high negative charge density, redundant primary sequence and low content of non-polar amino acids, which are other reasons for OPN to be an intrinsically disordered protein[39]. It is composed of 297 amino acids in mouse and 314 amino acids in human. OPN contains a number of domains thought to be critical for its function[38]. The primary sequence of OPN reveals a copious amount of charged residues, few hydrophobic residues and a high proportion of

disordered-promoting residues (D, M, K, R, S, Q, P and E). Serine, glutamic acid, glutamine, aspartic acid and asparagine comprise approximately one half of OPN's amino acid content.

Posttranslational modifications (PTMs) might have significant effects on the structure of the OPN molecule and on its biological properties [40], [13]. The most extensive PTM is phosphorylation of serine and threonine [41]. Rat bone OPN contains 12 phosphoserines and 1 phosphothreonine. The exact locations of the phosphate groups have revealed considerable heterogeneity. Thus, any given serine or threonine that was a substrate for an appropriate kinase may be partially phosphorylated, and the total number of phosphoserines would be fewer than the total number of potential sites. In contrast, bovine milk OPN appears to be maximally phosphorylated, wherein 27 phosphoserines and 1 phosphothreonine have been identified [42]. The extent of phosphorylation of OPN may play an important role in its physiological function for example, in influencing hydroxyapatite formation[43].

OPN is known to participate in numerous physiological and pathological processes, including biomineralization, cancer metastasis, wound repair, inflammation, immunity and apoptosis [31]. Physiological or normal calcification occurs in skeletal tissues whereas pathological or abnormal calcification refers to those occurring in functional soft tissues [44]. At physical sites of biomineralization, OPN has been found to involve in the inhibition of HA formation and growth. Within bone, OPN is found at especially high concentration in cement lines, sites where new bone is deposited onto older bone during remodeling [45]. In this context, OPN is thought to coat HA in the newly mineralized bone to inhibit its further growth and maintain closed contact between the older bone and the newly deposited osteoid matrix by mediating matrix-mineral interactions [46]. Several studies have been confirmed that OPN plays important role in

protecting host cell from lysis by the alternative complement pathway, an evolutionary older complement-activation pathway.

Several analyses have determined OPN is among the most strongly unregulated genes in several mouse and human cancers. OPN has been shown to enhance cancer cells' ability to intravasate into blood vessels [47],[48]. Considerable amounts of both in vitro and in vivo data suggested that OPN is able to inhibit the spontaneous precipitation and/or aggregation of several calcium-rich mineral phases, hence decreasing the overall size of pathological precipitation [31].

Moreover, OPN is found as a major organic constituent of growing renal calculi. OPN content and expression level are related to coronary artery disease severity and degree of calcification, respectively. More recent investigation have shown that OPN is an inducible inhibitor of dystrophic vascular calcification in vivo, suggesting the enhanced OPN expression observed with increased vascular calcification is a physical adaption aimed at preventing further calcification [49].

1.2 Crystal and protein interaction

Interactions between proteins and biological crystal are believed to play a central role not only in determination of the location, type, orientation and growth habit (size and shape) of crystal in tissue such as bone and teeth but also in preventing or limiting mineral formation in soft tissues[50]. The chemistry of this unique organic-inorganic interface, composed of crystal surface containing a variety of lattice ions and substitutions, steps and other lattice dislocations,

its associated water and counterion layers, and complex protein structures with a wide range of functional groups, is still poorly understood. It has been shown that proteins extracted from a variety of mineralized tissues are able to selectively interact in *vitro* with certain crystal faces and not others [13]. This was previously demonstrated by observing changes in morphology of crystals in the presence of proteins as compared to those in the absence of proteins. The surface of a crystal typically possesses several distinct features on which protein adsorb differently [51]. Some studies suggested that a thin layer of proteins may be formed which acts as a dissolution barrier, restricting the access of H^+ to the crystal surface and preventing diffusion of Ca^{2+} and PO_4^{3-} ions away from the HA. Alternatively, the protein molecules may bind to sites of high energy on the crystal surface, preventing ion detachment from these sites.

It is well known that protein-adsorption behaviours can be controlled by substrate surface parameters. The chemical properties of the crystal surface play an important role in determining the efficiency of protein adsorption and the amount of protein adsorbed by interaction between the functional groups on substratum and proteins, and even the conformation of adsorbed proteins [52]. The chemical nature of the surface can induce greater protein–surface interactions through either electrostatic or hydrophobic interactions [51]. It is generally accepted that electrostatic force played a vital role in the protein adsorption process as has been proved by many experimental and computer simulation studies [53]. The charged ions or groups on the substrate surface can bond with the charged functional groups, including amino group, carbonyl group, and carboxylate group, etc., on the protein molecules to dominate the protein adsorption. The bonded ions or groups on substrate surface or proteins are generally called adsorption sites. Ca^{2+} is believed to be the protein-binding sites on Ca-P surfaces and provide the major driving force for protein adsorption. When the pH is 7.4, which is equal to that of the physiological

environment, acidic protein and basic protein carry a negative charge and positive charge, respectively. Thus, the electrostatic interaction between substrate surface and proteins could be affected by the surface charge and protein net charge in different solutions.

Proteins with negatively charged residues generally exhibit a high affinity for the surface of HA [15]. The propensity and clustering of these negative charges suggests that the high affinity of these protein and peptides toward calcium-rich minerals is derived from their ability to electrostatically interact with calcium ions. Poly-anionic proteins able to adsorb to the HA surface with high affinity have been observed to possess negative residues [54]. These proteins possess relatively high proportions of aspartic acid, glutamic acid, and phosphorylated serine residues. For instance, OPN is a phosphoglycoprotein of approximately 300 amino acids, many of which are aspartic or glutamic acids. It has been suggested that phosphate groups present in OPN make a large contribution to the protein-crystal binding property [48]. Thus, nonphosphorelated forms of OPN or OPN peptides are less inhibitory than the corresponding phosphorylated protein/peptide [55]. It is evident that phosphate groups present in OPN and other biomineral-associated proteins are required for crystal interaction. As a result, the combination of the importance of acidic residues and post-translational phosphorylation to biomineral adsorption indicate that negative charge is imperative to the ability of acidic protein and peptides to their function.

In the saliva the strongest precipitation inhibitors, are statherin and proline-rich [56] phosphoproteins (PRPs), both of which adsorb strongly to HA [12]. These molecules contain phosphoserine residues and have a significant number of negatively charged residues localized in their N-terminal regions, whereas the C-terminal regions contain mainly uncharged residues. The charged domains of both statherin and the PRPs have been shown to have high affinities for HA

surfaces. However, several other proteins containing charged domains may be moderate or weaker contributors to precipitation inhibition. The molecular mechanisms underlying statherin interaction with hydroxyapatite have been actively studied to define how proteins function at the inorganic mineral interface. The direct hydroxyapatite binding contacts have been generally ascribed to the acidic side chains and two phosphoserines at the N-terminus of statherin [12]. A similar study has shown that the N-terminus of statherin is responsible for anchoring the molecule to the HA surface by adopting an α -helix structure upon adsorption, although other regions of the molecule may be involved in stabilization of this adsorption [57]. Chen *et al.* suggested that there are two types of interactive mechanisms between an N-terminal 15-residue statherin-like peptide and HA [58]. One mechanism is related to the conformational change at lysine residue near to N-terminal from a helical structure to a random-coil structure. This mechanism is in agreement with Goobes *et al.*, who showed that the lysine residue was in close proximity to the HA surface [59]. Others suggested that it is an interaction of protein side chains at the lysine residue position and HA surfaces, forming a ‘network of hydrogen bonds’ that could be responsible for protein–mineral recognition[24]. It has also been shown that StN21, a synthetic peptide designed to have an amino acid sequence identical to the N-terminal of statherin, inhibits spontaneous and secondary precipitation of enamel [9]. StN21 is a stable peptide shown to effectively reduce mineral loss caused by erosion, thus possessing therapeutic potential.

1.3 Purpose of thesis

The potencies of OPN-derived peptides on HA dissolution were compared using *in vitro* pH-Stat method dissolution assay, which allows for prolonged steady-state crystal dissolution at pH 5.25. The main purpose of this study consists of two steps. The first step was to study phosphorylated residues on inhibiting HA dissolution and the second step was to examine the impact of highly acidic residues on inhibiting HA dissolution. All peptides have been compared on the basis of their 50% inhibitory concentration. The protein of most interest in this study is osteopontin, OPN. Synthetic peptides corresponding to amino acid 220-235 (pSHEpSTEQSDAIDpSAEK), P3, and amino acid 65-80 (pSHDHMDDDDDDDDGDD) ,POPAR , of rat bone OPN have been used. To achieve the first step, we studied; P3, which contains three phosphoserine residues, whereas P0 possess an identical amino acid sequence but lacks of phosphorylation. For the second step, we performed several tests using P-OPAR; and OPAR, both containing a block of consecutive aspartic acid residues. This peptide was used to elucidate whether the short poly-Asp sequence within OPN (9 consecutive Asp residues in rat OPN) is capable of adsorbing to HA and inhibiting the dissolution of HA.

In addition, we have used synthetic poly-L-aspartic (MW=2320) acid and poly-L-glutamic (MW= 2600) acids with different lengths in order to elucidate the role of the acidic residues on the HA dissolution of HA. Furthermore, the secondary structures of poly-aspartic acid and poly-glutamic acid have been studied using circular dichroism (CD) spectroscopy. The effect of statherin and its N-terminal 9-residue peptide, DR9, on HA dissolution has been studied in order to study whether the negative charge density and the helical conformation at the N-terminal region of statherin are important for its interaction with HA surfaces.

Chapter Two. pH-Stat method and dissolution studies

2.1 pH measurements in the Laboratory

Synthetic hydroxyapatite particles, films, coatings, fibers and porous skeletons are used extensively in various biomedical applications [60]. Since the chemical nature of natural hydroxyapatite and the inorganic phase of bones and teeth is almost the same, such different processes as; dental caries, osteoporosis; and in vivo biodegradation of artificial bone grafts might be simulated by dissolution of chemically pure calcium apatite in acids. Because the true dissolution mechanism of calcium apatite in acids appears to be of paramount importance, several models have been proposed to explain the processes. These models have provided important information about the factors associated with solution (pH, composition, saturation and hydrodynamics), bulk solid (chemical composition, solubility, particle sizes) and surface (defects, adsorbed ions, phase transformation) of the apatite crystals. Unfortunately, it is still impossible to obtain complete understanding for all the processes involved because experimental techniques able to provide direct following after diffusion, sorption, detachment and transformation of the single atoms, ions and molecules currently are lacking. For all dissolution methods, it is generally agreed that the steady-state conditions of apatite dissolution in aqueous acidic media include the following simultaneous processes or steps: (1) diffusion of chemical reagents from bulk solution to the solid/liquid interface; (2) adsorption of the chemicals onto the surface of apatite; (3) chemical transformations on the surface; (4) desorption of products (ions of fluoride, calcium and orthophosphate) from the crystal surface; and (5) their diffusion into the bulk solution.

However, the composition of in vivo systems cannot be controlled by the experiment to the same degree as the composition of purely chemical systems. In order to obtain more information

about the fundamental demineralization process in vivo and information about the influence of various components on these processes, one possible method is to study the process in vitro, in well-defined systems, in which the parameters needed for an adequate description can be determined; relatively easily. Parameters found to be important for the descriptions of in vitro, studied at biologically interesting concentration, pH, temperature and pressure ranges, should be taking into account in the study of the dissolution processes. The solubility of hydroxyapatite is greatly affected by the pH: in general, a more acidic environment causes hydroxyapatite to become more soluble, while a less acidic environment makes hydroxyapatite less soluble [61]. The critical pH is the pH at which a solution is just saturated with respect to a particular mineral, such as tooth enamel. Conversely, if the pH of the solution is lower than the critical pH, the solution is unsaturated, and the mineral will tend to dissolve until the solution becomes saturated. The concept of critical pH is applicable only to solutions that are in contact with a particular mineral, such as enamel. For instance, saliva and plaque fluid; are normally supersaturated with respect to tooth enamel because the pH is higher than the critical pH, so the teeth do not dissolve in the saliva or under plaque [62]. In addition, hydroxyapatite also contains several impurities such as carbonate which will increase HA solubility whereas fluoride will decrease solubility. Because the proportions of these impurities vary, and because the impurities can influence enamel solubility, that solubility of HA is not fixed. [63]

The pH-Stat is an automatic titrator configured to maintain the pH of a reaction mixture at a constant pH. Dissolution of dental hard tissue or HA consumes H^+ , so a strong acid, e.g. HCl, is added by the system to maintain constant pH, and the amount of H^+ consumed during an experiment can be measured. This method offers the advantage of accurate control over three important factors controlling dissolution: pH, temperature and stirring rate. The main advantage

of the pH-Stat as a technique in erosion research is the control of reaction pH (to better than ± 0.01 units). The stirring rate must be high to ensure good coupling of the system to the reaction. An automatic titrator set up to maintain a reaction at a constant pH by adding acid as appropriate. As the dissolution of hydroxyapatite consumes H^+ , the rate at which acid is added to maintain the pH at the chosen value is proportional to the rate of dissolution. This method allows observation of the dissolution process in real time, without needing to interrupt the process to make measurements. Efficient stirring is essential. The size of the stirring bar needs to be suitable for the volume of the solution and the speed as fast as possible without introducing air bubbles.

In recent years, the pH-stat method has been employed by many scientists laboratories for a wide range of applications. A pH-Stat study takes place as follows: (1) determining an optimum value for the pH of the studied reaction, (2) keeping the pH constant by adding a reagent to neutralise OH^- or H_3O^+ ions, (3) calculating the kinetics of the studied reaction based on the consumption of reagent required to keep the pH constant over time. The pH regulation of an experiment involves bringing the pH of the solution to the set value and maintaining the set pH by continually adding titrant [64].

HA is a form of calcium phosphate and both calcium and phosphate concentration and the pH are important determinations of the dissolution kinetic of HA. As a result, the aim of this part of the present study was to establish the pH value appropriate for the HA dissolution for our experiments. Critical pH is the term given to the highest pH at which there is a net loss of minerals from tooth enamel. Below the critical pH, HA will dissolve. As mentioned previously, dental enamel is composed primarily of HA but it also contains several impurities such as carbonate and fluoride. Because the proportions of these impurities vary from person to person,

and indeed from tooth to tooth, and because the impurities can influence enamel solubility, that solubility is not fixed and varies slightly from person to person. It has been shown that critical pH for the dissolution process is generally accepted to be 5.5 with slight change depending on individual factors. During the demineralization process, acid diffuses between the rods and reaches deeper areas of the enamel, where carbonated hydroxyapatite crystals are more susceptible to dissolution [65].

Because the pH in oral environment varies from near neutral to 5, the kinetics of dissolution of synthetic hydroxyapatite powders were studied at 37° C and constant pH in the pH range 5-6 by continuously recording proton uptake. The acid concentration was constant for all experiment (50 mM HCl). At pH 6, no dissolution was observed. In this chapter, addition HCl volume, which is proportional to the rate of dissolution, is plotted against pH. Each experiment was repeated several times because the pH- Stat method is highly sensitive to several parameters. As a result, dissolution experiments were made at pH 5.25 for 2 mg HA in 8 ml of final solution ,which will be mentioning in the following, for all experiments because of the moderate velocity of the dissolution process. The results have been presented in terms of H⁺ consumption during 60 minutes, in order to compare directly the results for different pH values.

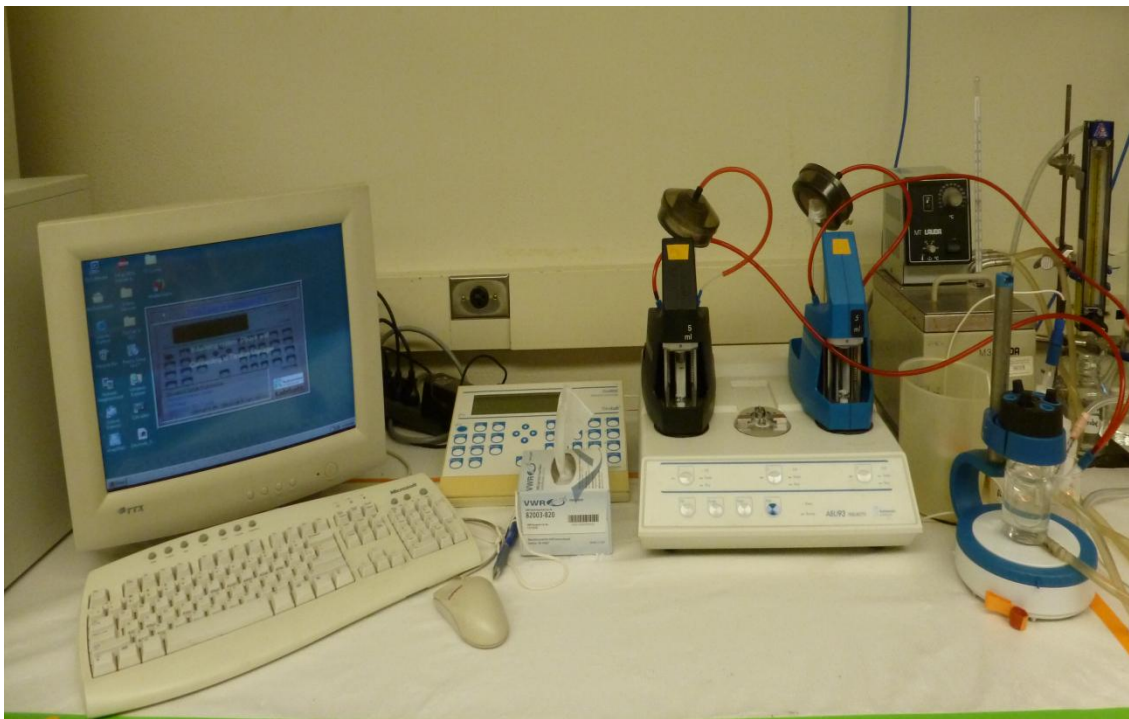


Fig 2. pH-Stat Titration Workstation

2.2 Materials and methods

2.2.1 Chemical and Reagents

Table 2. Chemical and Reagents

Ca (NO ₃) ₂ 4.H ₂ O (>99.0 %)	Sigma-Aldrich (St. Louis, MO)
NaCl (>99.5 %)	Sigma-Aldrich (St. Louis, MO)
NaOH (>98%)	EMD Chemical Inc. (Gibbstown, NJ)
HCl (36.5-38%)	EMD Chemical Inc. (Gibbstown, NJ)
Na ₂ HPO ₄	EMD Chemical Inc. (Gibbstown, NJ)
NH ₄ OH	Sigma-Aldrich (St. Louis, MO)
N ₂ (medical grade)	Praxair (Mississuga,ON)
0.2-µm Acrodisc Syringe Filter	PALL Corp. (Ann Arbor, MI)
Buffer Ph 7.000	Radiometer Analytical (Villeurbanne, FR)
Buffer Ph 10.012	Radiometer Analytical (Villeurbanne, FR)
Calomel Phc4006 electrode	Radiometer Analytical (Villeurbanne, FR)
TIM900 Titration Manager	Radiometer Analytical (Villeurbanne, FR)
ABU93 Triburette	Radiometer Analytical (Villeurbanne, FR)
TimTalk 9 version 2.1 software	LabSoft (Tampa,FL)

2.2.2 Synthesis of hydroxyapatite seed crystals

Hydroxyapatite for use in the constant-composition assay was synthesized by Azzopardi, 2010 using a modification of the protocol described by Nancollas and Mohan 1970 [66]. Briefly, 250 ml of 0.5 M $\text{Ca}(\text{NO}_3)_2$ was added drop-wise to magnetically stirred 250-ml solution of 0.3 M Na_2HPO_4 , which was maintained between pH 8.5 and 10 by the addition of concentrated NH_4OH (28-30% solution). The Na_2HPO_4 solution was also maintained at 70 °C whilst being bubbled with water-saturated nitrogen was bubbled to exclude atmospheric CO_2 . The precipitate was washed with H_2O , and then resuspended in mother liquor and refluxed for 24 h. The crystals were then washed in a medium sintered-glass funnel under vacuum, first with pH 10.0 H_2O then with acetone. The crystals were dried in a sealed Buchner flask under vacuum, and stored at room temperature in a desiccator.

2.2.3 Characterization of hydroxyapatite seed crystals

X-ray powder diffraction of the synthesized HA was utilized to verify the absence of other calcium phosphate phase. SEM of the synthesized HA revealed aggregates of plate/like crystals with apparent dimensions of approximately 2 nm in thickness, 40 to 200 nm in length and variable width.

The synthesized HA exhibits a Brunauer-Emmett-Teller (BET) surface area of 84.126 ± 0.094 m^2/g and a Langmuir surface area of 115.290 ± 2.347 m^2/g . ICP-AES analysis revealed the

calcium/phosphate molar ratio to be 1.612 ± 0.013 , in comparison to the theoretical ratio of 1.67 for HA.

2.3 HA- Dissolution assay

Metastable calcium phosphate solutions, called MCS solution, were prepared by combining 2 ml of H₂O (minus inhibitor volume), 4 ml of 8.8 mM Ca(NO₃)₂ and 2 ml of 8.8 mM Na₂HPO₄/200 mM NaCl (total volume 8 ml) and the inhibitor (dissolved in dH₂O) in a double-walled Pyrex vessel. These solutions were stirred and maintained at $37 \pm 0.1^\circ\text{C}$; using a circulating water bath connected to the Pyrex vessel. All the stock solutions were previously vacuum-filtered through 0.2- μm -pore-size membrane.

Five milliliter H₂O was combined with 20 mg HA powder, using first sonic bath and then magnetic stirrer. For each experiment, 0.5 ml of HA slurry in H₂O was used in order to have 2mg HA in 8 ml final solution. Water-saturated N₂ was bubbled through the solution to exclude atmospheric CO₂. The metastable solution was adjusted to pH 5.25 by adding small aliquots of 50 mM HCl or 50mM NaOH depending on the pH of the solution 30 minutes before adding HA. A calomel pHc4006 electrode connected to a TIM900 titration manager and an ABU93 triburette was immersed in the reaction solution. The probe was calibrated every day before each experiment with standard buffer solutions (pH 7.000 ± 0.01 and pH 10.012 ± 0.01) at 37°C.

The triburette was customized so that two of its 5-ml operated and both of which contained 50mM HCL. The titration manager was programmed to maintain pH 5.25 by adding acids for 60 minutes after addition of HA. Titration addition was controlled using Tim Talk 9 in pH-stat

mode with an endpoint pH 5.25 and proportional band pH of 0.100. The burettes were limited to a minimum speed of 1.0% /m and maximum speed of 3.0%/ min.

The reaction was initiated by adding of 0.5 ml of a made HA-H₂O slurry in H₂O, giving a final reaction solution composition of 2.2 mM Ca (NO₃)₂ , 2.2 mM Na₂HPO₄/ 50 mM NaCl.

As the reaction proceeds HA start to dissolve and OH ions are liberated which brings about to an increase pH of the reaction solution. The pH probe, programmed at 5.25, measures this change and sends a signal to pH monitor which dictates addition of titrants (HCL 50 mM) to the reaction by analytical burettes through autotitrator. The addition of titrants maintains pH at 5.25 during the experiment which is 60 minutes. The rate at which acid is added to maintain the pH at the chosen value is proportional to the rate of dissolution. The titration curve and the volume of titration solution consumed are recorded by computer. The HA dissolution rate, volume of HCl added to maintain pH, was compared to that observed in the absence/present of the tested peptides. Before using inhibitors several daily blank experiments (no peptide) have been run, to make sure that the result for control is consistent. Experiments were performed for various concentrations of peptides.

For all peptides HA dissolution rate, expressed as the volume of HCl addition for standard (no added protein/peptides) and with peptides, were plotted against protein/peptides concentration. The data for all were fitted to exponential decay curves using Prism 4 in order that the peptides could be compared on the basis of their 50% inhibitory concentration (IC₅₀). A representative example of a family of titration curves of HA growth rate in the presence of increasing concentrations of peptides will be illustrated. The slope of the linear portion of the HA dissolution assay decreased when higher concentration of peptides were used in the crystal dissolution assay. For all the experiments, there was a rapid addition of acid; lasting for < 10

min, immediately after HA was introduced into the solution. After this initial period, the acid addition is slow for 40 minutes and then for last the 10 minutes is almost constant. Both the initial rapid addition of acid and the slow period were highly variable between experiments because of the sensitivity of the pH-Stat method.

For each experiment, the dissolution rates with time were fitted to one site binding curves (hyperbola) (3) using Prism 4 (GraphPad, San Diego, CA).

$$Y=B_{max} * X / (K_d + X)$$

B_{max} is the maximum binding, and K_d is the concentration of ligand required to reach half-maximum binding.

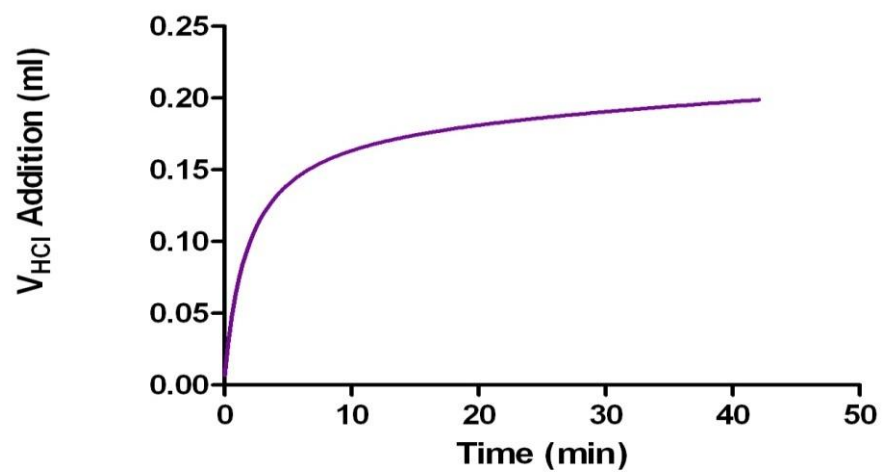


Fig 3. HCl addition required to maintain constant PH during the HA dissolution assay with 2 mg of hydroxyapatite in the MCS solution as it has been mentioned in dissolution assay .

The x-axis=time (min); y-axis=volume of titration added (ml)

Chapter Three- Protein inhibitory potency toward HA dissolution

3.1 Materials and methods

3.1.1 Chemical and Reagents

Table 3. Chemical and Reagents

Ca (NO ₃) ₂ 4.H ₂ O (>99.0 %)	Sigma-Aldrich (St. Louis, MO)
NaCl (>99.5 %)	Sigma-Aldrich (St. Louis, MO)
NaOH (>98%)	EMD Chemical Inc. (Gibbstown, NJ)
HCl (36.5-38%)	EMD Chemical Inc. (Gibbstown, NJ)
Na ₂ HPO ₄	EMD Chemical Inc. (Gibbstown, NJ)
NH ₄ OH	Sigma-Aldrich (St. Louis, MO)
N ₂ (medical grade)	Praxair (Mississuga,ON)
0.2-µm Acrodisc Syringe Filter	PALL Corp. (Ann Arbor, MI)
Buffer Ph 7.000	Radiometer Analytical (Villeurbanne, FR)
Buffer Ph 10.012	Radiometer Analytical (Villeurbanne, FR)
Calomel Phc4006 electrode	Radiometer Analytical (Villeurbanne, FR)
TIM900 Titration Manager	Radiometer Analytical (Villeurbanne, FR)
ABU93 Triburette	Radiometer Analytical (Villeurbanne, FR)
TimTalk 9 version 2.1 software	LabSoft (Tampa,FL)
Poly aspartic acid, Poly glutamic acid	Sigma-Aldrich (St. Louis, USA).

3.1.2 Peptides synthesis /purification

P3, P0, OPAR and P-OPAR peptides were synthesized and purified by Yinyin (Heidi) Liao and Kari Ann Orlay. Briefly, peptides were synthesized by a batch method with free amino acid and carboxyl termini using Fmoc chemistry and purified by high-performance liquid chromatography. All peptides purity was determined by mass spectroscopy and amino acid analysis. (Institute for Bimolecular Design, U of A/Advanced Protein Technology Center, SickKids). Statherin and DR9 were synthesized and purified in Dr Siqueira's laboratory in Western University Ontario.

3.1.3 Peptides secondary structure analysis

CD spectroscopy is a quantitative technique that can be used to estimate the fraction of residues in α -helix, β -strands, β -turn and disordered structures. CD studies were performed in our lab by Paul Azzopardi [48]. The secondary structure of the peptides were determined at 37°C from 250 to 190 nm, with a step size of 0.5 nm and a scan speed of 100 nm/min. P3, P0, OPAR and P-OPAR used in this study, were 16 residues in length. It has been confirmed in our Lab that all peptides used in this study exist predominantly in the disordered state in solution.

Poly aspartic acid and poly glutamic acid were suspended only in Po_4 because calcium is known to affect the secondary and tertiary structure of many proteins. However it has been shown in our laboratory that no major structure differences were observed in any of the peptides studied between the two buffers tested, one with calcium and another without calcium.

Table 4. Summary of the average fractional secondary structure of P3, P0,OPAR and P-OPAR

Peptide	Buffer*	Average	Fractional	Secondary	prediction [‡]
		α -Helix	β -strand	β -turn	Unordered
P3	Ca/PO ₄	3.6	15.2	9.2	71.5
	HEPES	2.3	15.9	9.2	72.1
P0	Ca/PO ₄	3.6	12.2	7.4	76.1
	HEPES	3.1	17.3	9.6	69.8
OPAR	Ca/PO ₄	4.1	27.6	14.6	53.0
	HEPES	3.5	23.1	13.1	59.7
P-OPAR	Ca/PO ₄	3.7	28.9	18.0	48.6
	HEPES	2.4	30.4	17.1	49.2

*Ca/PO₄buffer composition: 500 μ M Ca(NO₃)₂, 300 μ M Na₂HPO₄ and 150 mM NaCl, pH 7.40 HEPES buffer composition: 10 mM HEPES, 100 mM NaCl, 10 mM KCl, and pH 7.40, Azzaopardi (2009).

[‡] Reported fractional secondary structures are the average of those calculated using the CDSSTR and CONTINLL algorithms.

3.2 Inhibition of HA dissolution by OPN-derived peptides and statherin

The effect of OPN-sequence-derived peptides and the model compounds poly-Asp and poly Glu upon HA dissolution were evaluated using the pH-Stat method assay. HA dissolution rates were plotted against protein/peptide concentration. The data were fitted to exponential decay curve in order that the proteins could be compared on the basis of their 50% inhibitory concentration (IC_{50}).

P3 is the strongest inhibitor of HA dissolution in this study. The slope of linear portion of the HA dissolution assay decreased when higher concentrations of P3 was used in the dissolution assay. The IC_{50} for P3 was observed to be 6 $\mu\text{g/ml}$ - and complete inhibition of HA dissolution was achieved with 15 $\mu\text{g/ml}$. In contrast, P0's IC_{50} for HA dissolution was increased to approximately 75 $\mu\text{g/ml}$. The IC_{50} of P0 could not be measured precisely, as this peptide exhibited considerably reduced Inhibition compared to P3. IC_{50} for P3 is almost 10 times smaller than P0's IC_{50} suggesting that P3 strong inhibitory potency toward the HA dissolution. P-OPAR and OPAR exhibited IC_{50} 's of 16 $\mu\text{g/ml}$ and 22 $\mu\text{g/ml}$ respectively.

Poly-Asp (MW=2320) was observed to possess IC_{50} of 13 $\mu\text{g/ml}$ and completely inhibited crystal dissolution at a concentration of approximately 30 $\mu\text{g/ml}$. In contrast poly-Glu (MW=2600) exhibiting IC_{50} of 18 $\mu\text{g/ml}$.

Statherin (MW= 5380, 43 amino acid residues) and DR9 (MW= 1270 ,9-residue peptide derived from the N-terminal of the statherin) ,exhibited an IC_{50} of 25 μM and 13 μM respectively.

A representative example of a family of titration curves of HA dissolution rate in the presence of increasing concentration of all the peptides used in this study is illustrated.

Table 5. Summary of pH-Stat method dissolution result.

Peptide/ protein	# Residues	#PO ₄	#Acidic Residues	#Basic Residues	Net charge .¥	IC ₅₀ (µg/ml)
P3	16	3	5	1	-10	6
P0	16	0	5	1	-4	~75
P-OPAR	16	1	11	0	-13	16
OPAR	16	0	11	0	-11	22

¥ . Net charge =(-1 x #acidic residues)+(1 x #basic residues)+(-2x #phosphorylated residues)

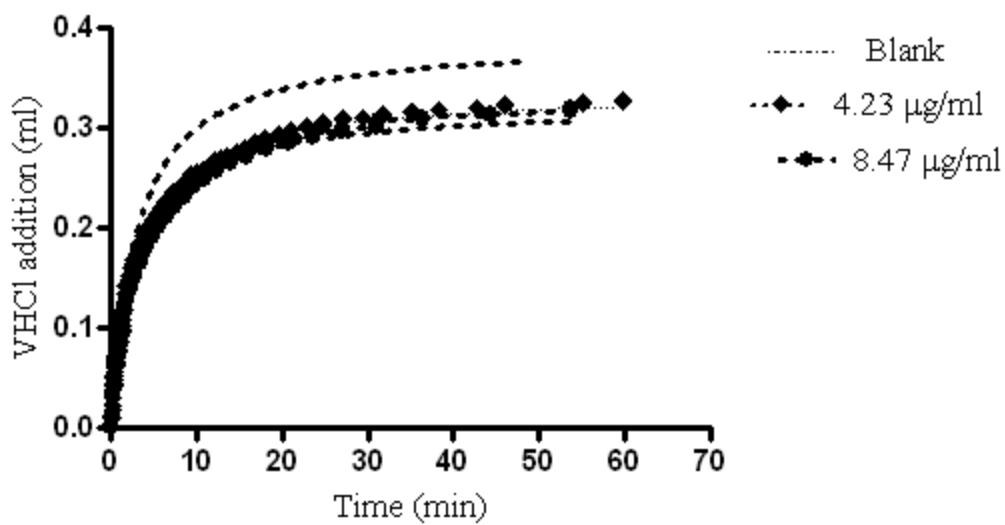


Fig 4. Initial rate of HA dissolution in the presence of increasing concentration of P0.

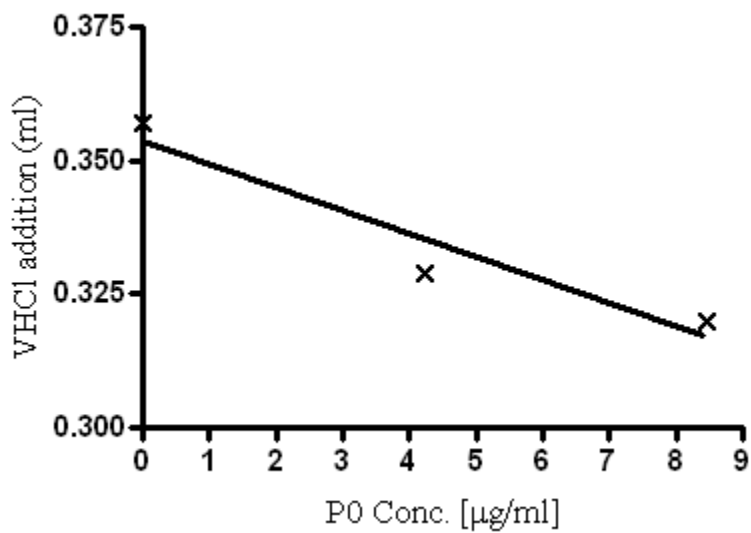


Fig 5. VHC1 addition against peptide Concentration (µg/ml). [$R^2=0.97$]

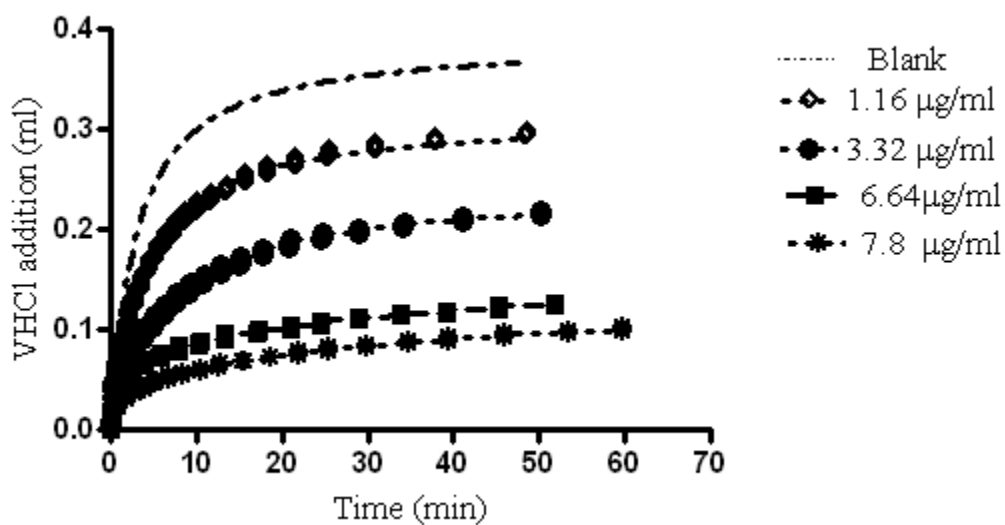


Fig 6. Initial rate of HA dissolution in the presence of increasing concentration of P3.

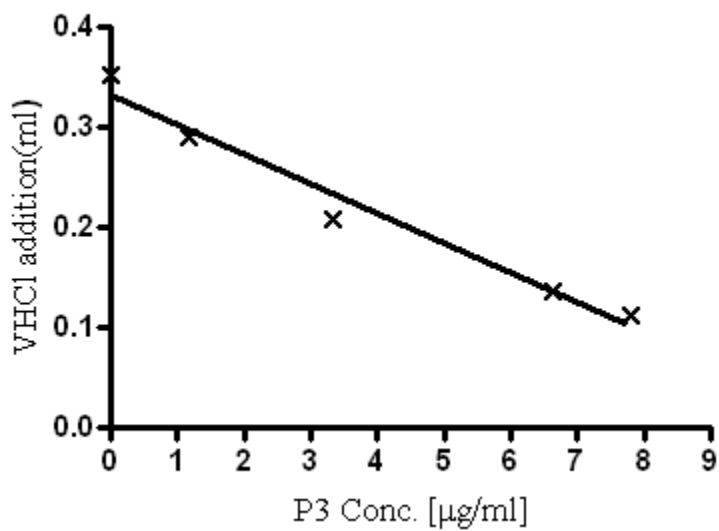


Fig 7. HCl addition against peptide Concentration ($\mu\text{g/ml}$). [$R^2 = 0.96$]

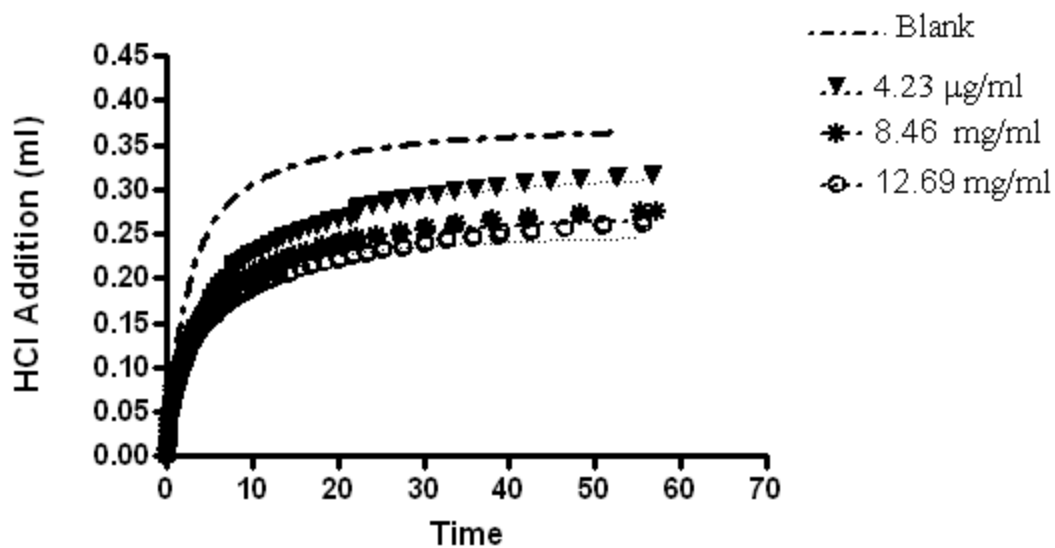


Fig 8. Initial rate of HA dissolution in the presence of increasing concentration of OPAR.

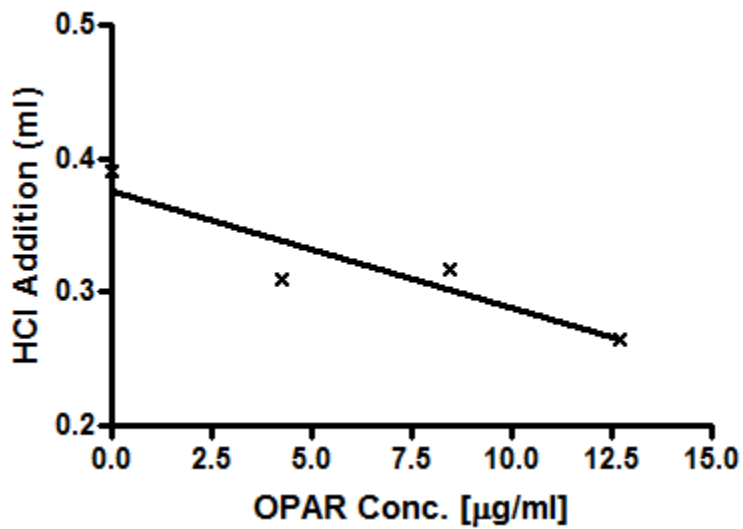


Fig 9. VHCl addition against peptide Concentration ($\mu\text{g/ml}$). [$R^2 = 0.85$]

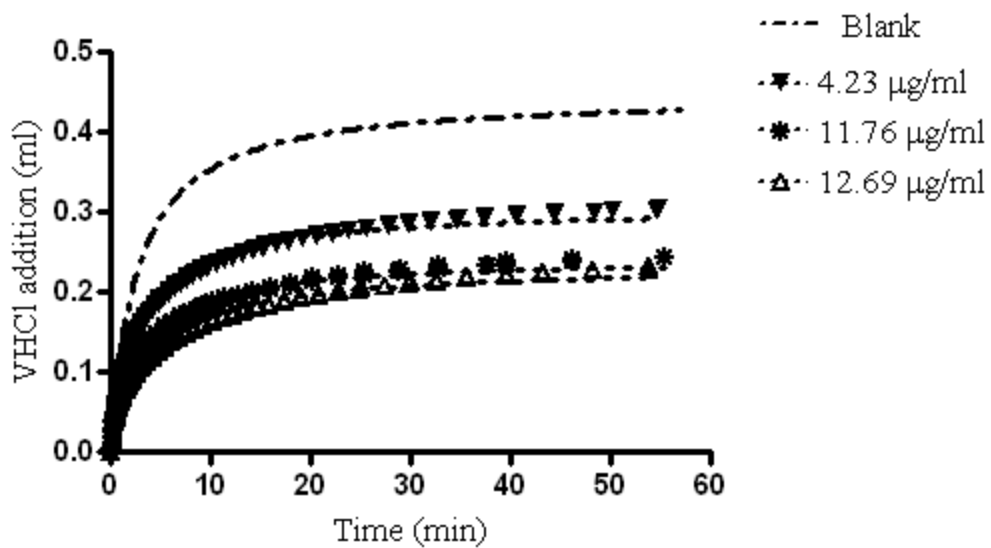


Fig 10. Initial rate of HA dissolution in the presence of increasing concentration of P-OPAR.

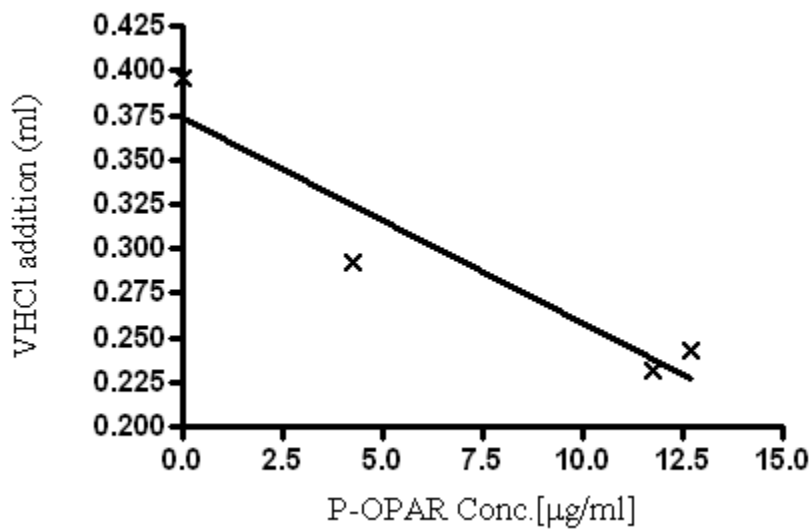


Fig 11. VHCI addition against peptide Concentration ($\mu\text{g/ml}$). [$R^2 = 0.89$]

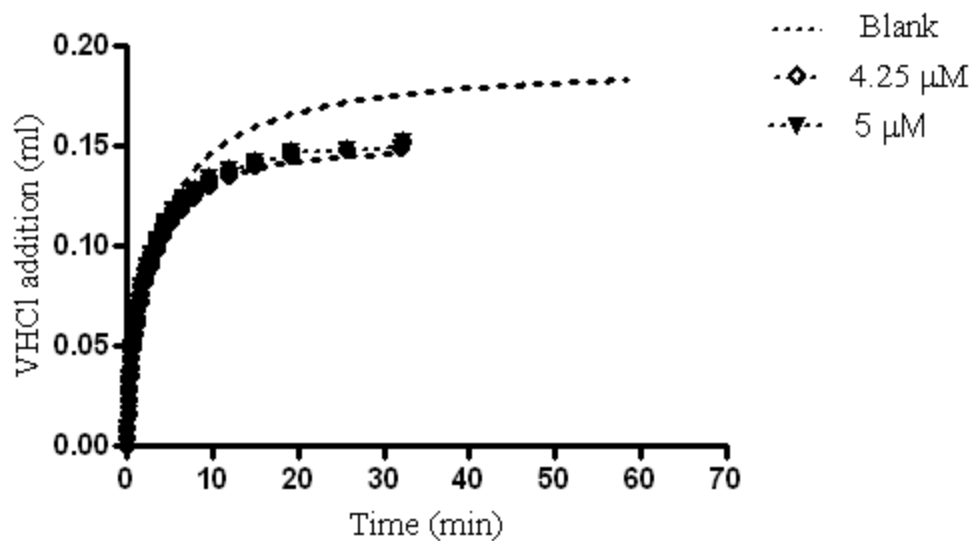


Fig 12. Initial rate of HA dissolution in the presence of increasing concentration of DR9.

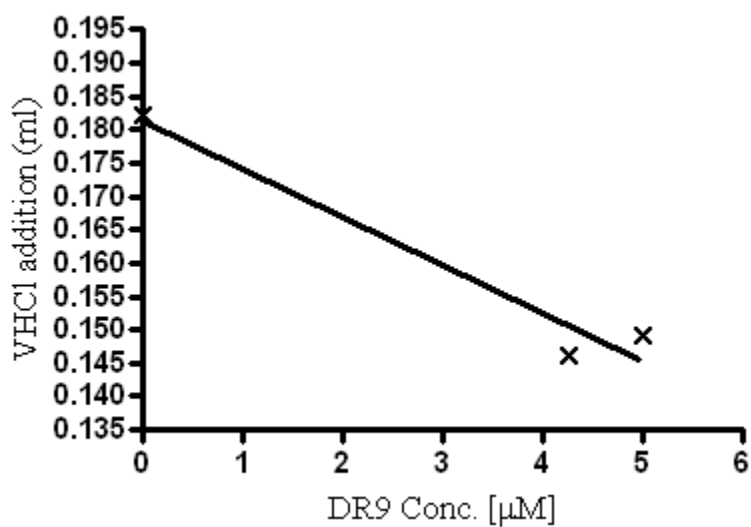


Fig 13. VHCl addition against peptide Concentration ($\mu\text{g}/\text{ml}$). [$R^2 = 0.96$]

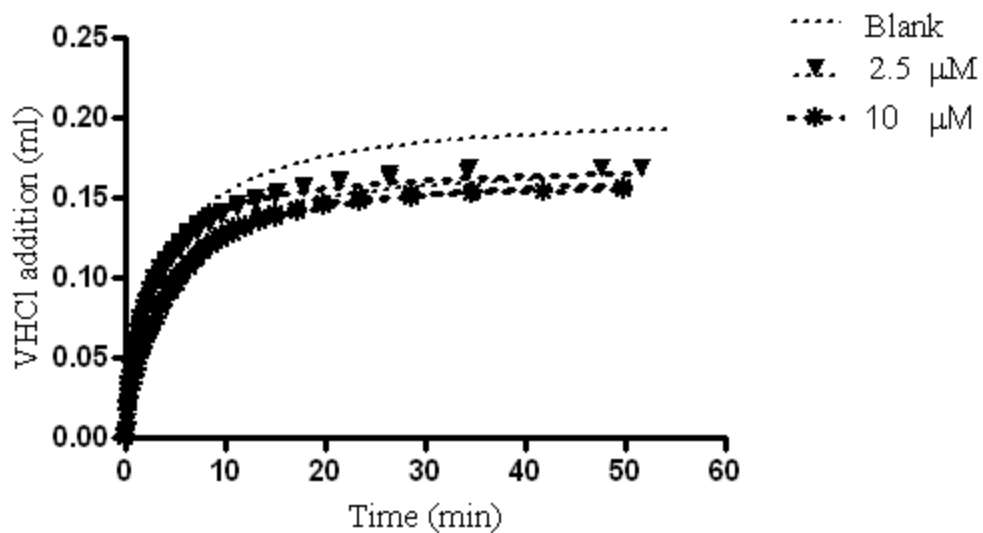


Fig 14. Initial rate of HA dissolution in the presence of increasing concentration of Statherin.

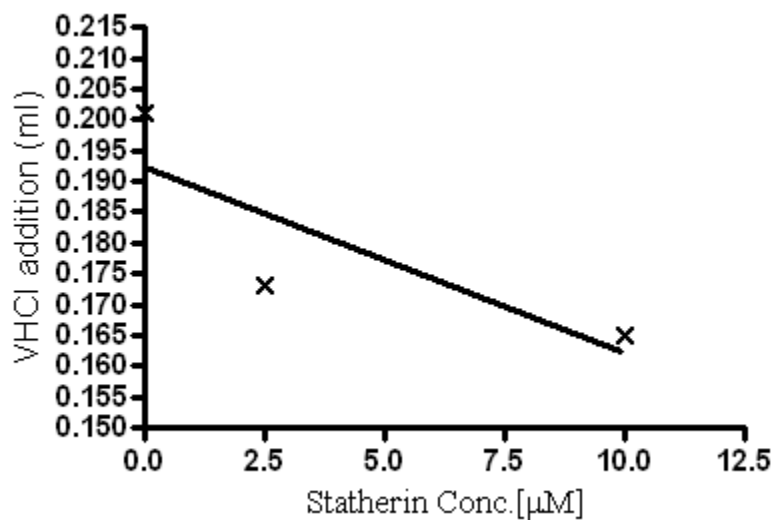


Fig 15. VHCl addition against peptide Concentration (μg/ml). [$R^2 = 0.81$]

3.3 Comparison between inhibitory potency of Aspartic and Glutamic acid

It has been shown that the amino acids interacting most closely with the face are aspartic and glutamic acid which are highly electronegative. Several studies have been directed towards the significance of acidic amino-acid residues in mineral-binding proteins since many members of this class are poly-anionic. The propensity of the negative charges suggested that the high affinity of acidic peptides toward calcium-rich mineral is derived from their ability to electrostatically interact with calcium ions. The consecutive short sequence of aspartic residues found in OPAR seems to confer a high degree of inhibitory potency toward HA dissolution. In the presence of P-OPAR the inhibition of HA dissolution increased slightly. It has been confirmed that the model compound poly-Asp, composed of consecutive acidic residues, has great affinity to HA surface. The pH-Stat assay showed that P3 is one of the strongest inhibitor of HA dissolution in this study. Examination of the equilibrium adsorption isotherm by Azzopardi in our laboratory showed that at saturation, approximately six times more P3 molecules are bound to the HA surface of HA than poly-Asp(11,000 Da). It has been suggested that this roughly correlates to the difference in mass between the two molecules, poly-Asp being approximately six times the mass of P3 and both, molecules bind to similar feature on HA and adsorb through a similar mechanism.

To determine the effect of poly-Glu and poly-Asp on the dissolution of HA, several experiments were performed in the experimental setup described previously. The poly-Asp and poly-Glu for this study both had the same length which is 20 amino acid. Poly-Asp (MW=2320) and poly-Glu (MW=2600) was observed to possess IC_{50} values of 13 $\mu\text{g/ml}$ and 18 $\mu\text{g/ml}$ respectively

A representative example of a family of titration curves of HA dissolution rate in the presence of increasing concentration of all the peptides used in this study is illustrated.

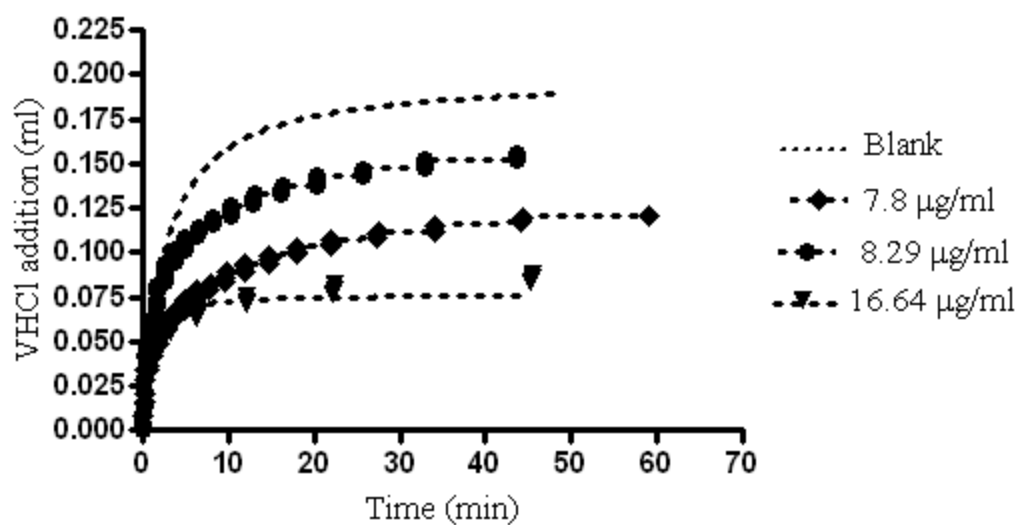


Fig 16. Initial rate of HA dissolution in the presence of increasing concentration of poly-Glu

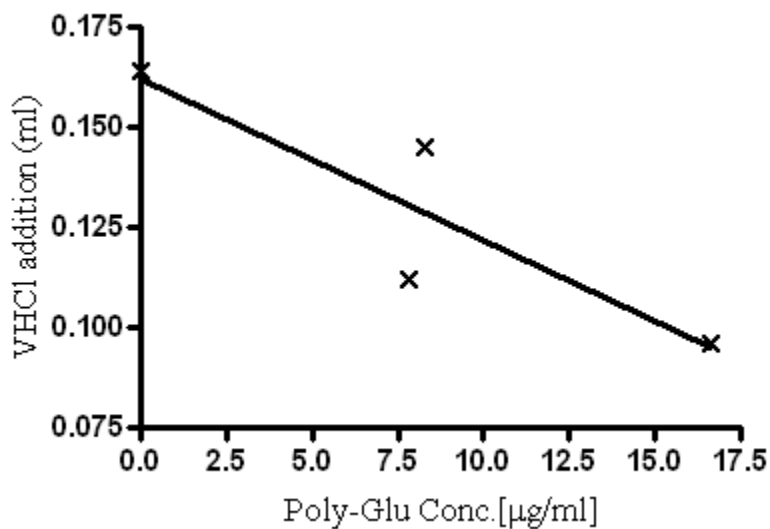


Fig 17. VHCI addition against peptide Concentration ($\mu\text{g/ml}$). [$R^2= 0.85$]

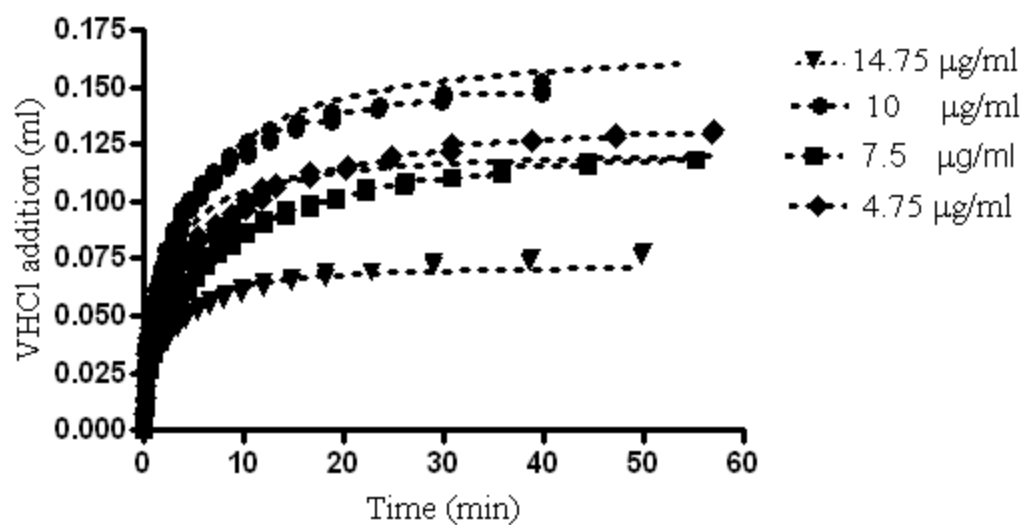


Fig 18. Initial rate of HA dissolution in the presence of increasing concentration of poly-Asp

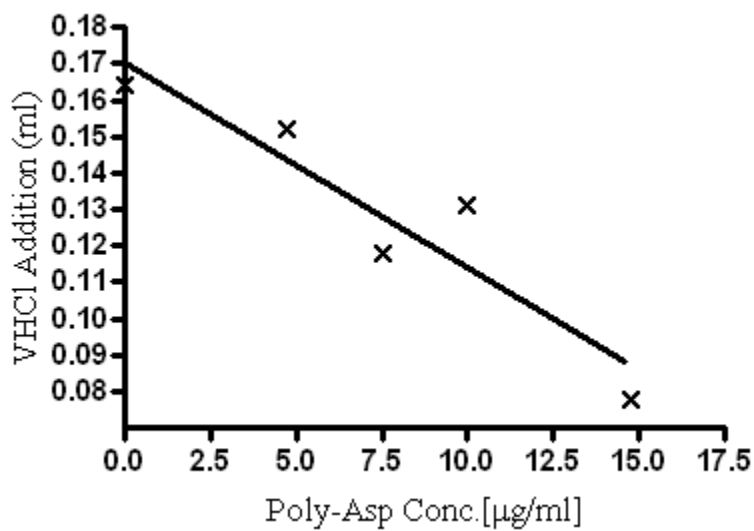


Fig 19. VHC1 addition against peptide Concentration (µg/ml). [$R^2 = 0.95$]

However, the secondary structures of these polypeptides may be quite different.

It has been confirmed that poly-L-glutamic acid has been shown to exist in the form of a left-handed "extended helix" at neutral and basic pH, and a right-handed α -helix at pH values low enough to protonate the carboxylate. poly-Asp has been reported to lack ordered secondary structure.

The secondary structures of the poly-Asp and poly-Glu were determined at 37°C in PO_4 buffer pH 5.25. All peptides analyzed by CD spectroscopy displayed the characteristic spectrum of a random coil secondary structure.

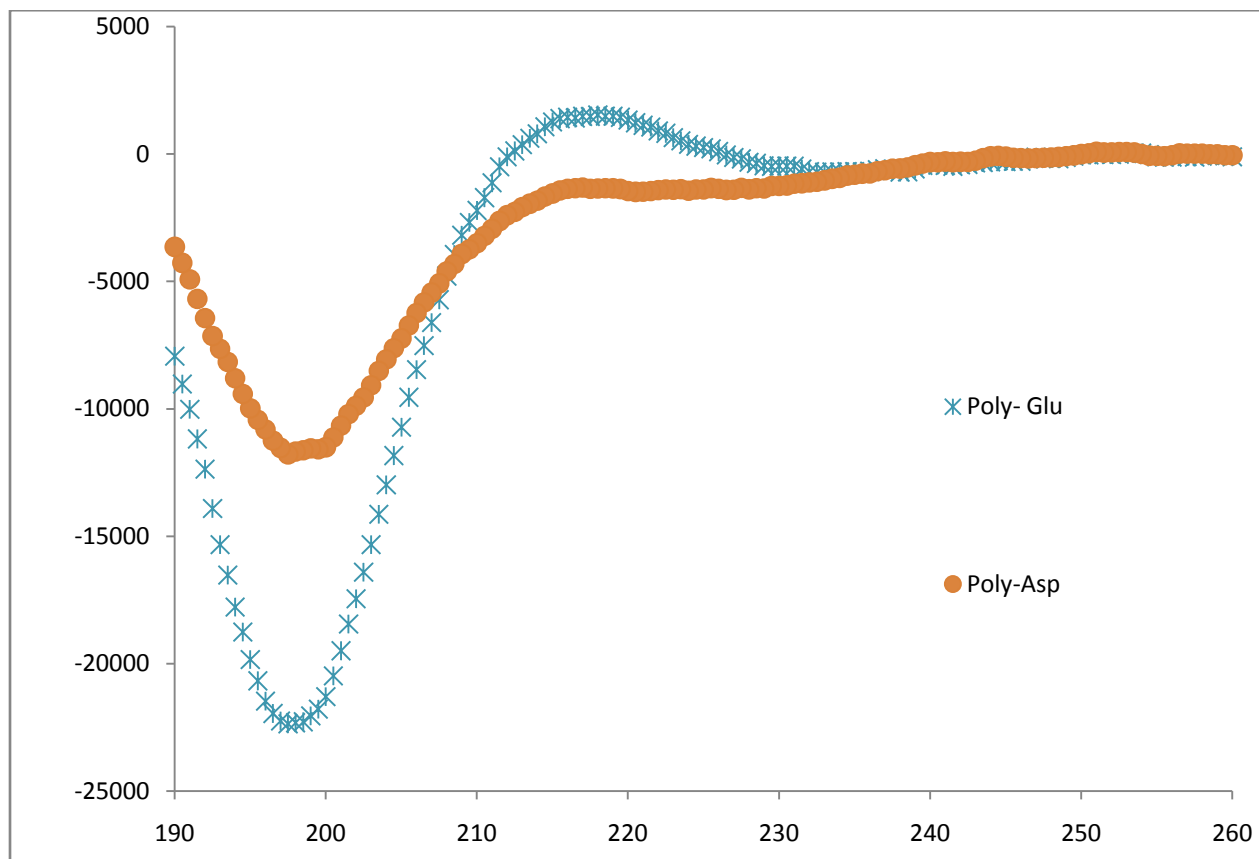


Fig 20. Poly-Asp and poly-Glu dissolved in PO_4 buffer used in pH-Stat experiments. CD spectra were collected at 37°C in 0.5-nm steps at a scan speed of 100nm/min.

3.4 Discussion

Dissolution experiments were performed using the pH-Stat method with 2 mg seed HA in 8 ml final solution as has been described previously and increasing concentrations of protein/peptide. The volume of the acid addition recorded during 60 min was used as the outcome variable. pH-Stat method revealed that the HA dissolution was composed of two distinct steps: an initial rapid addition of acid, lasting for < 10 min, immediately after HA was introduced into the solution, after which the acid addition decreases over the 30 minutes and then become constant up to at least 20 min. The transition to constant dissolution was found to occur within 20 minutes. Both the initial rapid addition of acid and the slow period were highly variable between experiments because of the sensitivity of the pH-Stat. All the experiments with the peptide and without peptide have been performed several times in order to make sure the results are consistent. Furthermore daily controls were run several time before running the experiment in the presence of peptides.

The effect of P3, P0, P-OPAR, OPAR, statherin and DR9 were evaluated using the pH-Stat dissolution assay at pH=5.25 for all experiments. Of the strong inhibitors, the inhibition potency of P3 > POPAR > OPAR > P0 when ranked according to their IC₅₀. P3 is the most potent inhibitor in this study, exhibiting IC₅₀ = 6 µg/ml. P3 contains three phosphoserine residues, whereas P0 possess an identical amino acid sequence but lacks phosphorylation. P0 exhibited considerably reduced inhibition compared to P3, exhibiting IC₅₀ > 75 µg/ml. Thus, the inhibitory potency of P0 was markedly increased by the addition of the 3 phosphate groups present in P3. These 3 phosphoserine residues collectively increase the magnitude of the negative charge by six (net charge of ~-10). We can assume, post-translational phosphorylation is able to increase potency of weak inhibitors. Although P0 is a weak inhibitor of HA dissolution, it has

been suggested that the regions adjacent to the poly-Asp region contribute to its inhibitory potency. Of the polypeptides tested, the strong inhibitors all possess a relatively high average net negative charge per residue. Consequently, the more negatively charged amino acids, the closer the protein can bind to the Ca^{2+} on the crystal's surface and as a result better inhibitor of HA dissolution.

Isothermal Titration Calorimetry (ITC) has been used to assess the thermodynamic of the P0, P3 and HA interaction in our laboratory by Azzopardi in 2009 [48]. It has been suggested that each peptide/protein likely has a distinct number of binding site for HA and it was necessary to elucidate the stoichiometry of each adsorbate-HA interaction prior to analysis by ITC. This was performed with series of equilibrium adsorption isotherm (EAI) experiments in which increasing amounts of peptide/ protein were equilibrated with a defined mass of HA crystals. The thermodynamic characterization was then performed subsequent to the elucidation of maximum number of binding sites (N_{max}) per unit surface area of HA for P3 and P0. It was observed that approximately six more times P3 binds to an equal mass of HA than P0. Utilizing a constant composition seeded-growth assay in our laboratory Azzopardi, showed that the crystal growth rate was reduced by approximately 80% at highest concentration of P3 tested (10 $\mu\text{g/ml}$) and P0 inhibited crystal growth by approximately 10% at highest concentration tested (15 $\mu\text{g/ml}$) [48]. The result of the current study aligns with our finding that the P3 is a strong inhibitor toward HA dissolution and growth suggesting that the 3 phosphoserines collectively increased the magnitude of the negative charge resulting a high affinity for HA surface. As a result, theoretically anything that inhibits crystal growth should also inhibit crystal dissolution.

P-OPAR and OPAR exhibited IC_{50} of 16 $\mu\text{g/ml}$ and 22 $\mu\text{g/ml}$ respectively. The consecutive short sequence of aspartic acid residues found in OPAR seems to confer a high degree of

inhibitory potency. In the presence of P-OPAR, the Inhibition of HA dissolution increased only slightly compared with OPAR. The phosphate clusters and blocks of consecutive aspartic acid residues are both able to effectively inhibit HA dissolution suggests that regions possessing concentrated negative charge are required to produce a robust inhibitor for the HA dissolution.

Of the polypeptides tested, the strong inhibitors all possess a relatively high average net negative charge per residues. It has been shown that the amino acids interacting most closely with the face are aspartic and glutamic acid which are highly negative.

To elucidate the effect of these acidic polypeptides, poly-L-Asp (MW=2320) acid and poly-L-Glu acid (MW=2600) , both 20 amino acid, have been studied using pH- Stat method. Poly-Asp and poly-Glu were observed to possess an IC_{50} of 13 $\mu\text{g/ml}$ and 18 $\mu\text{g/ml}$ respectively. Although both poly-Asp and poly-Glu relatively contain high average of negative charge per residues, they adsorb to the crystal with different property [48]. This finding suggested acquiring information regarding the secondary structures of poly-Asp and poly-Glu peptides using far UV circular dichroism.

Different explanation has been suggested toward different affinity of poly-Asp and poly- Glu to HA surface. It has been suggested that the reason that poly-Asp is a more effective inhibitor of poly-Glu binding than vice versa is that the binding of an anionic polypeptide to a crystal occurs when the binding of carboxylate group successively allows the polypeptide to "mold" itself to the spacing of counterions [46] . Poly-Asp, with its lack of secondary structure, should be easily capable of this; extended-helical poly-Glu less so. A difference in conformational flexibility may therefore explain why poly-Asp is a more effective inhibitor than poly-Glu toward HA dissolution. . As a result we assume that poly-Asp to have greater affinity to HA surface compare with poly-Glu with the same length.

Thus, strongly interacting areas tend to be disordered while weakly interacting areas tend to be ordered. It has been shown in our Lab that the highly disordered residues D, M, K, S, Q and E constitute 69% and 82% of P3/P0 and OPAR/P-OPAR respectively. As a result, they suggested that it is likely that these peptides, P3, P0, OPAR and P-OPAR, exist predominantly in the disorder state in solution. Thus, the closer a peptide associates with the crystal face, the better it inhibits crystal dissolution.

The N-terminus of statherin contains a pSpSEE (where pS is phosphorylated serine) acidic motif also have shown the inhibitory potency toward HA dissolution. Several studies showed that statherin inhibit formation of mineral precipitates on the tooth surface by inhibiting both spontaneous calcium phosphate precipitation and HA secondary crystal growth. Statherin can achieve these properties by binding calcium ions in solution and by adsorbing to HA surfaces with a significant binding affinity and coverage. The 2 phosphoserine residues present in N terminus of statherin (pSpSEE) produce a potent inhibitor, exhibiting IC_{50} of 25 μ M. DR9, also possess 2 phosphoserine which we think is the major component for its ability to interact with HA and inhibit further dissolution exhibiting 13 μ M.

REFERENCES

- [1] Wang L, Nancollas GH: "Dynamics of Biomineralization and Biode-mineralization." *Met Ions Life Sci* 2010, 4:413-456.
- [2] Dorozhkin SV, Epple M: "Biological and medical significance of calcium phosphates." *Angew.Chem Int Ed Engl* 2002, 41:3130-3146.
- [3] Lei Dang, Hukins DW, Wardlaw D. (2006) "Mechanical properties of calcium sulphate/hydroxyapatite cement". *Bio-Medical Materials and Engineering*;16(6):423–31.
- [4] Graves RC, Stamm JW: "Decline of dental caries. What occurred and will it continue?" *J Can Dent Assoc* 1985; 51: 693-699
- [5] Allenspach-Petrzilka, G.E. & Guggenheim , B. (1983). "Bacterial invasion of the periodontium; an important factor in the pathogenesis of periodontitis." *J Clin Periodontol* 10: 609-617.
- [6] Dawes C. (2003). "What is the critical pH and why does a tooth dissolve in acid?" *J Can Dent Assoc* 69(11):722-724.
- [7] Gorbunoff J. M. J." (1984) Interaction of proteins with hydroxyapatite". *Anal. Biochem.*, 136 425-445.
- [8] Lin Zhu, Jens Kreth, Sarah E. Cross, James K. Gimzewski, Wenyuan Shi, and Fengxia Qi. "Functional characterization of cell-wall-associated protein WapA in *Streptococcus mutans*." *A Journal of the Society for General Microbiology*.
- [9] Kosoric J, Williams RAD, Hector MP, Anderson P: "A synthetic peptide based on a natural salivary protein reduces demineralisation in model systems for dental caries and erosion". *Int J Pept Res Ther* 2007;4:497-503.
- [10] M. Hannig, N. J. Hess, W. Hoth-Hannig, and M. de Vrese, "Influence of salivary pellicle formation time on enamel demineralization-an in situ pilot study," *Clin. Oral Investig.* 7, 158–161 2003.

- [11] Van Nieuw Amerongen, A. and Veerman, E. C. I. (2002) "Saliva – defender of the oral cavity". *Oral Dis.* 8, 12–22
- [12] Schwartz, S. S., Hay, D. I. & Schluckebier, S. K. (1992) "Inhibition of Calcium Phosphate Precipitation by Human salivary Statherin". *Calcif.Tissue Int.*50,511–517.
- [13] Hoyer ,J.R., Asplin , J.R. and Otvos , L.(2001) "Phosphorylated osteopontin peptides suppress crystallization by inhibiting the growth of calcium oxalate crystals". *Kidney Int* 60, 77-82
- [14] Gorski JP." Acidic phosphoproteins from bone matrix: a structural rationalization of their role in biomineralization". *Calcif Tissue Int.* 1992;50(5):391–396.
- [15] Addadi, L. and Weiner, S. (1985). " Interactions between acidic proteins and crystals: stereochemical requirements in biomineralization." *Proceedings of the National Academy of Science*, 82, 4110-4114.
- [16] Douglas WH, Reeh ES, Ramasubbu N et al. (1991). "Statherin: a major boundary lubricant of human saliva". *Biochem. Biophys. Res. Commun.*180 (1): 91–7.
- [17] Hay DI, Smith DJ, Schluckebier SK, Moreno EC. "Relationship between concentration of human salivary statherin and inhibition of calcium phosphate precipitation in stimulated human parotid saliva." *J Dent Res.* 1984 Jun;63(6):857–863.
- [18] Humphrey SP, Williamson RT. "A review of saliva: normal composition, flow, and function." *J Prosthet Dent.* 2001;85:162-169.
- [19] Lamkin MS, Oppenheim FG. "Structural features of salivary function". *Crit Rev Oral Biol Med* 1993; 4: 251–259.
- [20] Ferguson DB." The salivary glands and their secretions" , oral bioscience. Edinburgh: Churchill-Livingstone, 1999; 118–150.
- [21] Sreebny, L.M. (2002) "Saliva in health and disease: an appraisal and update". *Int. Dent. J.* 50, 140-161

[22] Socransky, S. S. & Haffajee, A.D. (2002). "Dental biofilms: difficult therapeutic targets, Periodontol" 2000 28:12-55.

[23] Jensen JL, Lamkin MS, Oppenheim FG. " Adsorption of human salivary proteins to hydroxyapatite: a comparison between whole saliva and glandular salivary secretions."J. Dent. Res. 1992; 71:1569.

[24] Goobes G, Goobes R, Gibson JM, Long JR, Paranjli R, Popham JM, Raghunathan V, Shaw WJ, Campbell CT, Stayton PS, Drobny GP." The structure, dynamics, and energetics of protein adsorption-lessons learned from adsorption of statherin to hydroxyapatite. "Mag. Res. Chem. 2007;45:S32–S47.

[25] Bahar, G; Feinmesser, R; Shpitzer, T; Popovtzer, A; Nagler, RM (2007). "Salivary analysis in oral cancer patients: DNA and protein oxidation, reactive nitrogen species, and antioxidant profile". Cancer 109 (1): 54–59

[26] Goobes R, Goobes G, Campbell CT, Stayton PS. " Thermodynamic roles of basic amino acids in statherin recognition of hydroxyapatite."Biochemistry 2006; 45: 5576

[27] Hay, D. I., and Oppenheim, F. G. (1974). " The isolation from human parotid saliva of a further group of proline-rich proteins" Arch. Oral. Bid. 19, 627-32

[28] Long JR, Shaw WJ, Stayton PS, Drobny GP. " Structure and dynamics of hydrated statherin on hydroxyapatite as determined by solid-state NMR. "Biochemistry. 2001 Dec 25;40(51):15451-5.

[29] Qin C, Baba O, Butler WT. "Post-translational modifications of sibling proteins and their roles in osteogenesis and dentinogenesis. " Crit Rev Oral Biol Med. 2004 Jun 4;15(3):126-36. Review.

[30] Schedlbauer, A., Ozdowy, P., Kontaxis, G., Hartl, M., Bister, K., and Konrat, R. (2008) "Backbone assignment of osteopontin, a cytokine and cell attachment protein implicated in tumorigenesis". Biomol. NMR Assignments 2 (1), 29–31.

- [31] Rittling, S.R. and Denhardt, D.T. (1999) "Osteopontin function in pathology: lesson from osteopontin deficient mice. *Exp Nephrol* 7, 103-113
- [32] Fisher , L.W. and Fedarko , N .s. (2003) "Six genes expressed in bones and teeth encode the current members of the SIBLING family of proteins " *Connect tissu Res* 44 Suppl 1, 33-40
- [33] G.K. Hunter, H.A. Goldberg. " Modulation of crystal formation by bone phosphoproteins. Role of glutamic acid-rich sequences in the nucleation of hydroxyapatite by bone sialoprotein." *Biochem J*, 15 (1994), pp. 175–17
- [34] Rangaswami H, Bulbule A, Kundu GC (February 2006). "Osteopontin: role in cell signaling and cancer progression". *Trends Cell Biol.* 16 (2): 79–87
- [35] Fisher LW, Fedarko NS (2003). "Six genes expressed in bones and teeth encode the current members of the SIBLING family of proteins". *Connect. Tissue Res.* 44 Suppl 1: 33–40.
- [36] Christensen B, Nielsen MS, Haselmann KF, Petersen TE, Sørensen ES (August 2005). "Post-translationally modified residues of native human osteopontin are located in clusters: identification of 36 phosphorylation and five O-glycosylation sites and their biological implications". *Biochem. J.* 390 (Pt 1): 285–92
- [37] Wang KX, Denhardt DT (2008). "Osteopontin: role in immune regulation and stress responses". *Cytokine Growth Factor Rev.* 19 (5-6): 333–45.
- [38] Crosby, A.H., Edwards, S.J., Murray, J.C., Dixon, M.J. (May 1995). "Genomic organization of the human osteopontin gene: exclusion of the locus from a causative role in the pathogenesis of dentinogenesis imperfecta type II". *Genomics* 27 (1): 155–160.
- [39] Boskey AL (1992) "Mineral-matrix interactions in bone and cartilage". *Orthop. Relat. Res* 281: 244–274.
- [40] P.J. Neame, W.T. Butler . "Posttranslational modification in rat bone osteopontin" *Connect Tissue Res*, 35 (1996), pp. 145–150

- [41] Goldberg, H.A., Warner, K. J., Stillman, M. J. and Hunter, G. K. (1996). "Determination of the hydroxyapatite-nucleating region of bone sialoprotein". *Connect tissue Res.* 35, 385- 392
- [42] E.S. Sorensen, P. Hojrup, T.E. Petersen. "Posttranslational modifications of bovine" *Prot Sci*, 4 (1995), pp. 2040–2049
- [43] Goldberg,H.A. and Hunter, G.K (1995) "The inhibitory activity of osteopontin on Hydroxyapatite formation in vitro". *Ann N Y Acad Sci* 760, 305-308
- [44] Steitz SA, Speer MY, McKee MD, Liaw L, Almeida M, Yang H, Giachelli CM (2002)."Osteopontin inhibits mineral deposition and promotes regression of ectopic calcification".*Am. J. Pathol.* 161 (6): 2035–46.
- [45] Choi ST, Kim JH, Kang EJ, Lee SW, Park MC, Park YB, Lee SK (2008). "Osteopontin might be involved in boneremodelling rather than in inflammation in ankylosing spondylitis". *Rheumatology (Oxford)* 47 (12): 1775–9.
- [46]Goldberg HA, Warner KJ, Li MC, Hunter GK. "Binding of bone sialoprotein, osteopontin and synthetic polypeptides to hydroxyapatite". *Connect Tissue Res.* 2001;42(1):25–37
- [47] Wang KX, Denhardt DT (2008). "Osteopontin: role in immune regulation and stress responses". *Cytokine Growth Factor Rev.* 19 (5-6): 333–45.
- [48] P.V. Azzopardi, J. O’Young, G. Lajoie, M. Karttunen, H.A. Goldberg and G.K. Hunter (2010): "Roles of electrostatics and conformation in protein-crystal interactions." *PLoS One* 5(2), e9330 (DOI 10.1371/journal.pone.0009330)
- [49] Mei Y.Speera, Yung-Ching Chienb, Mary-Quana, Hsueh-Ying Yanga, Hojatollah Valib, "Smooth muscle cells defecient in osteopntin have enhance susceptability to calcification in vitro". *Cardiovascular Research* 2005 662(2):324-333
- [50] Norde W., Anusiem A. C. I. 1992 "Adsorption, desorption and re-adsorption of proteins on solid surfaces". *Colloids Surf.* 66, 73–80.

- [51] Hay D. I., Moreno E. C. 1979 "Differential adsorption and chemical affinities of proteins for apatitic surfaces." *J. Dent. Res.* 58, 930–942
- [52] Proctor GB, Hamdan S, Carpenter SH, Wilde P. "The structure, dynamics, and energetics of protein adsorption". *Biochem. J.* 2005; 389: 111.
- [53] Stayton PS, Drobny GP, Shaw WJ, Long JR, Gilbert M. "Molecular recognition at the protein-hydroxyapatite interface". *Crit Rev Oral Biol Med* 2003; 14: 370–376.
- [54] Giachelli CM, Steitz S. "Osteopontin: a versatile regulator of inflammation and biomineralization." *Matrix Biol* 2000;19:615-622.
- [55] Fejerskov O, Kidd E, eds. "Dental Caries: The Disease and its Clinical Management". 2nd ed. Oxford, United Kingdom: Blackwell Munksgaard; 2008.
- [56] Hay DI, Carlson ER, Schluckebier SK, Moreno EC, Schlesinger DH. "Inhibition of calcium phosphate precipitation by human salivary acidic proline-rich proteins: structure-activity relationships". *Calcif Tissue Int.* 1987 Mar;40(3):126–132.
- [57] Raj PA, Johnsson M, Levine MJ, Nancollas GH. "Dependence on sequence, charge, hydrogen bonding potency, and helical conformation for adsorption to hydroxyapatite and inhibition of mineralization". *J Biol Chem* 1992; 267: 5968–5976.
- [58] Chen PH, Tseng YH, Mou Y, Tsai YL, Guo SM, Huang SJ, Yu SSF, Chan JCC. "Adsorption of a statherin peptide fragment on the surface of nanocrystallites of hydroxyapatite". *J Am Chem Soc* 2008;130:2862–2868.
- [59] Goobes G, Stayton PS, Drobny GP. "Solid state NMR studies of molecular recognition at protein-mineral interfaces". *Prog Nucl Magn Reson Spectrosc* 2007; 50: 71–85.
- [60] A. Bigi, E. Boanini, M. Gazzano, K. Rubini, P. Torricelli. "Nanocrystalline hydroxyapatite-polyaspartate composites". *Bio-Med Mater Eng* (2004) 14, 573 – 579
- [61] Fejerskov O, Kidd E, eds. "Dental Caries: The Disease and its Clinical Management". 2nd ed. Oxford, United Kingdom: Blackwell Munksgaard; 2008.

[62] Shannon IL, Suddick RP, Dowd FJ Jr. "Saliva: composition and secretion." Monogr Oral Sci. 1974 Jun;2:1-103.

[63] Deakins M, Volker IF. "Amount of organic matter in enamel from several types of human teeth." J Dent Res 1941;20(2):117-21.

[64] Tanford, C. (1962). "The interpretation of hydrogen ion titration curves of proteins." Adv. Prot. Chem. 17,69-165

[65] Wikiel K, Burke EM, Perich JW, Reynolds EC, Nancollas GH." Hydroxyapatite mineralization and demineralization in the presence of synthetic phosphorylated pentapeptides." Arch. Oral Biol.1994;39:715-721.

[66] Nancollas GH, Mohan MS (1970) "The growth of hydroxyapatite crystals". Arch. Oral Biol 15: 731-745.